EUMETSAT

NWC SAF

SUPPORT TO NOWCASTING AND VERY SHORT RANGE FORECASTING

Scientific and Validation Report for the iSHAI Processors of the NWC/GEO

NWC/CDOP3/GEO/AEMET/SCI/VR/iSHAI, Issue 1, Rev.0

21 January 2019

Applicable to GEO-iSHAI v4.0 (NWC-032)

Prepared by Agencia Estatal de Meteorología (AEMET)

REPORT SIGNATURE TABLE

Function	Name	Signature	Date
Prepared by	Miguel A. Martinez (AEMET)		*21 January 2019*
Reviewed by	Xavier Calbet, AEMET (NWC SAF GEO Manager) NWC/GEO v2018 DRR Review Board		*21 January 2019*
Authorised by	Pilar Ripodas, AEMET (NWC SAF Project Managers)		*21 January 2019*

DOCUMENT CHANGE RECORD

Version	Date	Pages	CHANGE(S)
1.0	*21 January 2019*	58	Updated version after NWC/GEO v2018 DRR.
1.0d	*31 October 2018*	58	Draft for version 2018 DRR

TABLE OF CONTENTS

List of Tables and Figures

1. INTRODUCTION

The Eumetsat "Satellite Application Facilities" (SAF) are dedicated centres of excellence for processing satellite data, and form an integral part of the distributed EUMETSAT Application Ground Segment (http://www.eumetsat.int).

This documentation is provided by the SAF on Support to Nowcasting and Very Short Range Forecasting, hereafter NWC SAF. The main objective of NWC SAF is to provide, further develop and maintain software packages to be used for Nowcasting applications of operational meteorological satellite data by National Meteorological Services. More information can be found at the NWC SAF webpage, http://nwc-saf.eumetsat.int. This document is applicable to the NWC SAF processing package for geostationary meteorological satellites, NWC/GEO.

1.1 SCOPE OF THE DOCUMENT

The purpose of this document is to present the Scientific Validation results for the Clear Air Product Processor of the NWC/GEO package version 2018. The name of Clear Air Product Processor is GEO-iSHAI (imaging Satellite Humidity And Instability).

The scientific validation for GEO-iSHAI version 2018 outputs has been mainly based on the validation of the GEO iSHAI parameters using as input synthetic RTTOV SEVIRI brightness temperatures and real bias corrected SEVIRI brightness temperatures. In the Section 2 and 3, all GEO-iSHAI coefficients and the validation figures have been calculated from the GEO iSHAI validation datasets using temporally and spatially collocated real SEVIRI and synthetic RTTOV brightness temperatures (calculated using profiles from ECMWF GRIB files on hybrid levels).

The case with synthetic BTs inputs is used to draw the main characteristics of the retrievals. The case using as input real bias corrected SEVIRI BTs is used to show the deviation from the theoretical one in operational conditions and to advice users on the limitation of the algorithm. To be able to make global validation and given that ECMWF analyses are of high quality, in this report these fields are taken as ground truth parameters.

In Section 4 it has been started the validation of AHI instrument on board Himawari using only synthetic RTTOV simulation from the SEVIRI GEO-iSHAI validation and training dataset but simulated with RTTOV using the AHI channels coefficients. In CDOP-3 more specific AHI and ABI Scientific Reports using real AHI and ABI BTs will be written. Same it will made for validation of GEO-iSHAI with ABI instrument on board GOES-R class. These AHI and ABI validations will be made on best-effort basis and with limited period looking for the comparison of the GEO-iSHAI validation with the validation of similar products from the Japanese Meteorological Agency and NOAA.

Within this document, from now on GEO-iSHAI will only be referring to version 2018.

1.2 SOFTWARE VERSION IDENTIFICATION

The validation results presented in this document apply to the GEO iSHAI version 4.0 product. This GEO-iSHAI version is included in the version 2018 of NWC/GEO software package.

1.3 GLOSSARY

Please refer to the "Nowcasting SAF Glossary" document in the NWC SAF web for a wider glossary and a complete list of acronyms for the NWC SAF project.

ABI	Advanced Baseline Imager
AEMET	Agencia Estatal de Meteorología Meteorology State Agency (Spain)

AHI	Advanced Himawari Imager
ASCII	American Standard Code for Information and Interchange
ATBD	Algorithm Theoretical Basis Document
BL	Precipitable water in low layer (P_{sfc} – 850 hPa)
BT	Brightness Temperature
CDOP (CDOP-1)	Continuous Development and Operations Phase (1)
CDOP-2	Continuous Development and Operations Phase 2
CDOP-3	Continuous Development and Operations Phase 3
CF	NetCDF Climate and Forecast (CF) Metadata Conventions
CIMSS	Cooperative Institute for Meteorological Satellite Studies (USA)
CMa	Cloud Mask
COTS	Commercial-Off-The-Shelf
CPU	Central Processor Unit
DEM	Digital Elevation Model
ECMWF	European Centre for Medium-range Weather Forecasts
EOF	Empirical Orthogonal Function
EUMETSAT	European Organisation for the Exploitation of Meteorological Satellites
FCI	Flexible Combined Imager (MTG)
FG	First Guess
FOV	Field Of View
FOR	Field Of Regard
GEO	Geostationary Satellites
GEO-CMa	GEO Cloud Mask and Cloud Amount
GEO-iSHAI	GEO imaging Satellite Humidity And Instability
GRIB	Gridded Information in Binary Form
HDF5	Hierarchical Data format version 5
HL	Precipitable water in High Layer (500 – 0 hPa)
hPa	Hecto Pascal
HRIT	High Rate Image Transmission
IDL	Interactive Data Language
IR	InfraRed
IREMIS	InfraRed Emissivity
IRS	Infrared Sounder (MTG)
iSHAI	imaging Satellite Humidity And Instability
K	Kelvin
KI	K-Index
km	kilometre
LI	Lifted Index
LPW	Layer Precipitable Water

LST	Land Surface Temperature
MARS	ECMWF Meteorological Archive and Retrieval Facility
McIDAS	Man Computer Interactive Data Access System
ML	Precipitable water in Medium Layer (850 – 500 hPa)
MSG	Meteosat Second Generation
MTG	Meteosat Third Generation
MTG-FCI	Meteosat Third Generation Flexible Combined Imager
MTG-IRS	Meteosat Third Generation Infra Red Sounder
netCDF	Network Common Data Form
NRT	Near Real Time
NWC	Nowcasting
NWC/GEO	Geostationary part of the Nowcasting SAF
NWCLIB	Nowcasting Library
NWCSAF	Nowcasting SAF
NWP	Numerical Weather Prediction
NWP SAF	SAF for Numerical Weather Prediction
LPW	Layer Precipitable Water
PGE	Product Generation Element PGE01 Cloud Mask (GEO-CMa) Product Generator PGE13 SEVIRI Physical Retrieval (SPhR) Product Generator
PW	Precipitable Water
RTM	Radiative Transfer Model
RTTOV	Radiative Transfer for TOVs
SAF	Satellite Application Facility
SEVIRI	Spinning Enhanced Visible InfraRed Imager
SG	Steering Group
SHAI	Satellite Humidity And Instability
SHW	Showalter Index
SKT	Skin Temperature
SST	Sea Surface Temperature
SW	Software
TOZ	Total ozone
TPW	Total Precipitable Water
TM	Task Manager
UM	User Manual
VR	Validation Report
VSA	Visiting Scientist Activities
WV	Water Vapour Channel

1.4 REFERENCES

1.4.1 NWC SAF Applicable Documents

The following documents, of the exact issue shown, form part of this document to the extent specified herein. Applicable documents are those referenced in the Contract or approved by the Approval Authority. They are referenced in this document in the form [AD.X]

For versioned references, subsequent amendments to, or revisions of, any of these publications do not apply. For unversioned references, the current edition of the document referred applies.

Current documentation can be found at the NWC SAF Helpdesk web: http://nwc-saf.eumetsat.int.

Ref.	Title	Code	Vers
[AD.1]	Proposal for the Third Continuous Development and Operations Phase (CDOP-3) March 2017-February 2022	NWC SAF: CDOP-3 proposal	1.0
[AD.2]	Project Plan for the NWCSAF CDOP3 phase	NWC/CDOP3/SAF/AEMET/MGT/PP	1.0
[AD.3]	Configuration Management Plan for the NWC SAF	NWC/CDOP3/SAF/AEMET/MGT/CMP	1.0
[AD.4]	NWC SAF Product Requirements Document	NWC/CDOP3/SAF/AEMET/MGT/PRD	1.0
[AD.5]	Interface Control Document for Internal and External Interfaces of the NWC/GEO	NWC/CDOP3/GEO/AEMET/SW/ICD/1	1.0
[AD.6]	Data Output Format	NWC/CDOP3/GEO/AEMET/SW/DOF	1.0
[AD.7]	System and Components Requirements Document for the NWC/GEO	NWC/CDOP2/GEO/AEMET/SW/SCRD	2.1
[AD.8]	NWC SAF CDOP-3 Project Plan Master Schedule	NWC/CDOP3/SAF/AEMET/MGT/PP/MasterSchedule	1.1
[AD.9]	Component Design Document for the NWCLIB of the NWC/GEO	NWC/CDOP2/GEO/AEMET/SW/ACDD/NWCLIB	2.0
[AD.10]	Interface Control Document for the NWCLIB of the NWC/GEO	NWC/CDOP3/GEO/AEMET/SW/ICD/2	1.0
[AD.11]	User Manual for the Tools of the NWC/GEO	NWC/CDOP3/GEO/AEMET/SCI/UM/Tools	1.0

Table 1: List of Applicable Documents.

The reference documents contain useful information related to the subject of the project. These reference documents complement the applicable ones, and can be looked up to enhance the information included in this document if it is desired. They are referenced in this document in the form [RD.X]

For dated references, subsequent amendments to, or revisions of, any of these publications do not apply. For undated references, the current edition of the document referred applies.

1.4.2 Reference Documents

Ref.	Title	Code	Vers	Date
[RD.1]	Validation Report for "PGE13 SEVIRI Physical Retrieval" (SPhR– PGE13 v1.2)	SAF/NWC/CDOP2/INM/SCI/VR/11	1.0	15/02/12
[RD.2]	Scientific Report: improvements in "PGE13 SEVIRI Physical Retrieval Product (SPhR)" using as input ECMWF GRIB files on hybrid levels	SAF/NWC/CDOP2/INM/SCI/RP/02	1.0	15/07/13
[RD.3]	Algorithm Theoretical Basis Document for iSHAI Product Processors of the NWC/GEO	NWC/CDOP2/GEO/AEMET/SCI/ATBD/iSHAI	2.1	21/01/19
[RD.4]	User Manual for iSHAI Product Processors of the NWC/GEO: Science Part	NWC/CDOP3/GEO/AEMET/SCI/UM/ iSHAI	1.0	21/01/19
[RD.5]	Scientific and Validation Report for the Clear Air Product Processor of the NWC/GEO	NWC/CDOP2/GEO/AEMET/SCI/VR/ClearAir	1.0	15/10/16

Table 2: List of Referenced Documents

Note: [RD.5] is the Validation Report of GEO-iSHAI version 2016.

2. SEVIRI GEO-ISHAI VALIDATION DATASET

2.1 DESCRIPTION OF FILES USED

Validation is continuous and important task for us. The construction of the training and validation dataset was started in 31 December 2007; since the resolution and files has evolved with time, in this document the ones used in this Validation Report are described.

In order to build the GEO-iSHAI datasets for training and validation purposes, real data from MSG SEVIRI images and ECMWF GRIB files have been used. The period used in the Validation Report is 2017. Since December 2016, the daily request to MARS has been reconfigured with a broader region and with the request also of the t+24 forecasts as described below.

At the time of writing this report the input data files available for training, tuning and validation activities are:

From ECMWF fields:

- 00 Z and 12 Z runs
- analysis (*t+00* hours) and (*t+12* hours) and (*t+24* hours) forecasts
- region: global for absolute latitude less than 65º. That is NW corner at (65º N, 180º W) and SE corner at (65º S, 179.8º E). In previous report [RD.5] the ECMWF GRIB files were generated using region NW corner at (65º N, 65º W) and SE corner at (65º S, 65º E). Now, the broad region allows to generate training and validation dataset with other GEO satellites than the operational MSG at 0º with slight modifications of the code.
- time period: from 31 December 2016 12 Z to present of each day during this period. The database is updated every day.
- horizontal resolution: 0.2º by 0.2º
- vertical resolution: two different vertical resolutions are used
    - Hybrid levels (hereafter denoted as NWP-Hyb): The number is 137 levels.
    - Fixed pressure levels (hereafter denoted as NWP-P): These GRIB files are needed only for Cloud Mask (CMa) processing. The pressure levels available on MARS are typically 15 or 25 synoptic levels (as example: 1000, 925, 850, 700, 500, 400, 300, 250, 200, 150, 100 .. hPa)

      Note: the NWP-P GRIB files are the ones used as input to the NWCSAF software package and needed here just for CMa generation.
- parameters: temperature (T) profile, humidity profile (specific humidity [q] for NWP-Hyb and relative humidity [RH] for NWP-P files), ozone profile, skin temperature.

Note: when the collocated records are written, the NWP(t+24) from previous 24 hours ECMWF run, the NWP(t+12) from previous 12 hours ECMWF run are collocated in the same record with the NWP(t+00). As example, the 01 January at 00UTC NPW(t+00) analysis profile is collocated in the same record than the one with the NWP(t+24) from 31 December 00 UTC run and the NWP(t+12) from 31 December 12 UTC run.

From MSG SEVIRI Observations:

- 00 Z and 12 Z slots
- region: frame of 3400 x 3400 IR pixels centred at subsatellite position (only pixels with satellite zenith angle lower than 70º)
- time period: from 1 January 2008 00 Z to present of each day during this period (continuous update) but in this Validation Report it has been used the 2017 year
- horizontal resolution: SEVIRI full resolution and MSG projection

- SEVIRI channels: All SEVIRI channels but HRVIS
- Currently in the validation datasets there are MSG data from MSG-1, MSG-2, MSG-3 and MSG-4. In this report the period selected is the year 2017 and for this reason MSG-3 is the satellite used when real SEVIRI brightness temperatures (hereafter BTs) are used.

These are the dynamic information datasets used for the tuning and validation activities. Specific datasets used for different objectives are in part generated from them and descriptions are provided in the respective sections.

2.2 DESCRIPTION OF PROCESS TO GENERATE THE VALIDATION DATASET

To build one good validation and training dataset is a high priority and standing task for us. The process to build the GEO-iSHAI v2018 validation dataset is a heritage of the process used to build the PGE13 SPhR validation dataset (see [RD.1] or [RD.2]) and GEO-iSHAI version 2016 validation dataset (see [RD.5]).

The main idea is to generate the whole validation dataset using the NWCGEO Cloud Mask (CMa) program and a modified version of GEO-iSHAI from NWSAF/MSG v2016 software called PGE00 which also uses RTTOV-11.2 for an efficient generation of collocated real and synthetic BTs.

PGE00 and GEO-iSHAI allow activating an option in their configuration files to write at clear pixels in optional binary files structures with real SEVIRI BTs together with the T, q and O_3 profiles, surface and ancillary parameters collocated spatially, temporally and vertically interpolated to the position and time of the clear SEVIRI pixels. The optional binary files of GEO-iSHAI just save the MSG IR channels used in iSHAI algorithm; but PGE00 is configured to save the full set of 8 MSG IR channels.

The use of RTTOV-11.2 implies that the GEO-iSHAI validation dataset is based on profiles with 54 pressure levels. It has been used NWC/GEO v2016 GEO-CMA and GEO-iSHAI. Thus, all the profiles used in the validation have similar characteristics to the profiles used and retrieved within the GEO-iSHAI v2018 execution in operational mode.

The 2017 year has been chosen as the reference period for the GEO-iSHAI validation dataset. The validation results obtained using as ground truth the ECMWF NWPHyb analysis (*t+00*) profiles are presented here. In section 3, the validation results using as input to GEO-iSHAI real bias BT corrected SEVIRI BTs are also included in order to show the deviation from the theoretical ones and to advice users on the limitation of the algorithm.

To avoid using for validation the same records as the ones used for calculation of the GEO-iSHAI 2018 version coefficients, the records with 1 out 3 offset 1 in the complete dataset have been used for validation.

Positions of GEO iSHAI validation dataset: For GEO iSHAI parameters validation, a set of predefined positions of a 1º x 1º grid plus the RAOB stations positions have been chosen. The set contains 13001 points in the actual mask. The positions where validation is made can be seen in Figure 1.

Process to build the GEO iSHAI validation dataset: The actual process to build the validation and training dataset is the following:

a) Calculate Cloud Mask (GEO-CMa): the cloud mask generation is the first step. The GEO-CMA program is first executed. The results of GEO-CMA program are netCDF files with the cloud mask located at *$SAFNWC/export/CMA*.

Please, note that for CMa the NWP GRIB files used as input need to be on fixed pressure levels whilst for this Validation Report all calculations come from hybrid ECMWF GRIB files (137 hybrid levels in 2017). In this report all background NWP profiles have been downloaded from ECMWF.

Note: In near future this step will be migrated to GEO-CMA version 2018.

b) Selection of clear validation locations by screening the cloud mask: the CMa cloud mask file is overwritten with the multiplication of CMa mask with the 13001 validation position mask (1 for selected pixel and 0 in the rest). The use of this screened cloud mask speeds up later the GEO-iSHAI and PGE00 process because instead of executing the physical retrieval over several millions of clear air pixels it is executed only over the clear air pixels among the 13001 predefined positions.

The process to get the screened cloud mask is:

- the cloud mask matrix is read from the CMa file
- the cloud mask matrix is multiplied with the 13001 validation positions mask (matrix with same dimensions of CMa with values: 1 for validation points and 0 for the rest of pixels) and the result is the screened cloud mask.
- This screened cloud mask is used to overwrite the CMa cloud mask netCDF file on *$SAFNWC/export/CMA*.

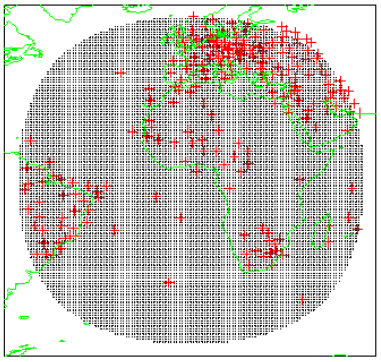

Figure 1: Predefined set of 13001 validation points used in validation datasets. Grid network of 1º x 1º plus Radiosonde Stations (red crosses).

c) To obtain the collocated profiles from analysis (*t+00*), (*t+12*) forecast and (*t+24*) forecast: the PGE00 program is executed three times for each slot. The PGE00 program calculates the profiles by interpolating the ECMWF fields from hybrid levels to 54 levels in the vertical and also in time and space. It also calls RTTOV-11.2 to calculate the synthetic BTs.

In the first PGE00 execution: the screened cloud mask, the real SEVIRI image and as background NWP the ECMW *t+00* analysis GRIB file (hereafter denoted as NWPH00) are used as inputs.

In the second PGE00 execution: the screened cloud mask, the SEVIRI image and as background NWP-Hyb the *t+12* forecast ECMWF GRIB file from previous 12 hour ECMWF run (hereafter denoted as NWPH12) are used as inputs.

In the third PGE00 execution: the screened cloud mask, the SEVIRI image and as background NWP the ECMW *t+24* forecast ECMWF GRIB file (hereafter denoted as NWPH24) are used as inputs.

In the first execution it is read the (T, q, O_3) profiles and some surface parameters at the clear air predefined positions from ECMWF *t+00* analysis.

With the second execution it is read the (T, q, O_3) profiles and some surface parameters (P_{sfc}, T_{skin}, etc), from the `$SAFNWC/tmp` binary files, at the clear air predefined positions from *t+12* hours ECMWF forecast.

With the third execution it is read the (T, q, O_3) profiles and some surface parameters (P_{sfc}, T_{skin}, etc), from the `$SAFNWC/tmp` binary files, at the clear air predefined positions from *t+24* hours ECMWF forecast.

Together with the *t+00*, *t+12* and *t+24* profiles, ancillary data (as emissivities, longitude, latitude, zenith angle, etc) are also read from the `$SAFNWC/tmp` binary files. The process (for (*t+00)* and *(t+12)* cases) can be seen in Figure 2. The result is one binary file by slot that can be easily read on IDL with the *restore* command. The mean number of retained clear pixels by slot is 4829.

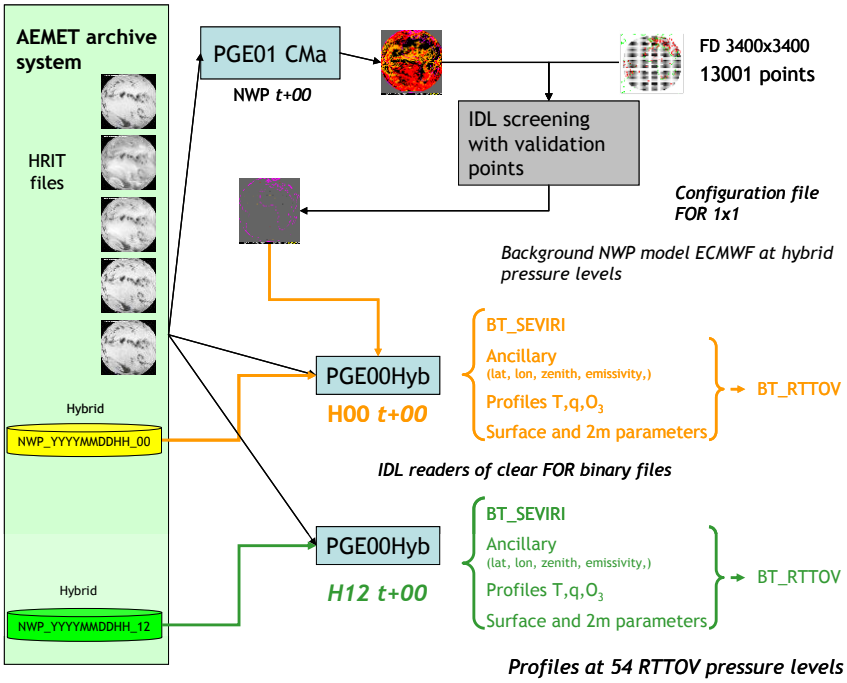

Figure 2: Generation of the records for adding to GEO iSHAI validation dataset from one image for (t+00) and (t+12) cases.

d) Joining the files for every slot on monthly files: In order to allow an easy management of the datasets, the slot binary files are joined in one file for every month. It is made with one IDL procedure. This monthly binary files are the base for the validation process since files on a monthly basis can be joined easily to build a wider period dataset.

e) Joining the monthly files on a period file: Once a period is selected for validation or training, one period binary file is generated joining the monthly files for the months in the period. It is made with one IDL procedure. In this validation report it has been used 1 out 3 clear pixels for the 2017 year. The number of pixels used here is 1,139,717 pixels. Other reason to use 1 out 3 of the 2017 clear pixels is that is needed only 2.5 GB; greater files could create memory problems in processing the validation chain.

f) Write binary file which can be used as input to the validation version of GEO-iSHAI: One array with selected parameters is written on a binary file in a format that will be used later with the ad hoc version of GEO-iSHAI for validation. This validation version processes the data record by record instead of processing a region of a satellite image, as is done in the GEO-iSHAI operational version.

g) Execute the ad hoc validation version of the GEO-iSHAI software: to get an assessment of the new coefficients for the First-Guess (hereafter FG) regression and the physical retrieval steps of 2018 GEO-iSHAI, one ad hoc validation version of the sources of GEO-iSHAI to process iSHAI algorithm and RTTOV-11.2 on record by record basis has been developed. Thus, it is possible to test the new FG regressions coefficients, Empirical Orthogonal Function (EOF) coefficients files, E^{-1} and B^{-1} matrices, avoiding the huge task to reprocess from the complete HRIT SEVIRI files and ECMWF GRIB files.

This also allows to choose as input to the algorithm real SEVIRI BTs (bias corrected or uncorrected) or synthetic RTTOV SEVIRI BTs. The outputs of this validation program are the profiles after FG regression and/or physical retrieval steps using as inputs the GEO-iSHAI validation dataset profiles. This process allows testing new version of iSHAI software or new coefficients just over GEO-iSHAI validation dataset before implementing it in the GEO-iSHAI operational software. This process is a natural consequence from previous experiences.

For version 2018 ad hoc variants for AHI (on board Himawari satellites) and ABI (on board GOES-R class satellites) instruments has been developed. The validation result for AHI variant in synthetic RTTOV case are shown in Section 4.

h) Build the GEO iSHAI validation dataset: The outputs of the previous step are blended with the structures of the validation dataset (ancillary fields as emissivity values, land/sea mask, height, etc.) and one IDL binary file for restoring is generated.

Structure of the records in the GEO iSHAI validation dataset: After the execution of the previous steps the validation dataset for a period is one array (that could contains several millions of records) written on an IDL binary file. The array can be restored easily with the use of IDL command *restore*. Every record is one IDL structure with the following parameters or fields:

- ***Ancillary***: longitude, latitude, emissivity values, etc.
- ***Date***: day, year, hour, etc.
- ***NWP from ECMWF analysis (t+00):*** ECMWF temperature and humidity profiles interpolated to the 54 RTTOV pressure levels interpolated vertically from 137 hybrid levels, T_{skin}, pressure at surface, etc. from the analyses (*t+00*) ECMWF GRIB files. It will be used as the validation truth.
- ***NWP from ECMWF forecast (t+12):*** ECMWF temperature and humidity profiles interpolated to the 54 RTTOV pressure levels interpolated vertically from 137 hybrid levels, T_{skin}, pressure at surface, etc. from the previous run to the image ECMWF *t+12* forecast (as example for image 20170101 at 00Z the *t+12* forecast from 20161231 at 12 UTC ECMWF run is used).
- ***NWP from ECMWF forecast (t+24):*** ECMWF temperature and humidity profiles interpolated to the 54 RTTOV pressure levels interpolated vertically from 137 hybrid levels, T_{skin}, pressure at surface, etc. from the previous run to the image ECMWF *t+24* forecast (as example for image 20170101 at 00Z the *t+24* forecast from 20161231 at 00 UTC ECMWF run is used).
- ***BT_SEVIRI(8)***: uncorrected BT from HRIT file. *BT_SEVIRI[IR3.9,WV6.2, WV7.3, IR10.8, IR8.7, IR9.7, IR12.0, IR13.4]*.
- ***SEVIRI BT_RTTOV(8) from NWPHyb(t+00)***: Synthetic BTs calculated using the RTTOV-11.2 with the analysis (*t+00*). *H00.BT_RTTOV[IR3.9,WV6.2, WV7.3, IR10.8, IR8.7, IR9.7, IR12.0, IR13.4]*.
- ***SEVIRI BT_RTTOV(8) from NWPHyb(t+12)***: Synthetic BTs calculated using the RTTOV-11.2 with the forecast (*t+12*). *H12.BT_RTTOV[IR3.9,WV6.2, WV7.3, IR10.8, IR8.7, IR9.7, IR12.0, IR13.4]*.
- ***SEVIRI BT_RTTOV(8) from NWPHyb(t+24)***: Synthetic BTs calculated using the RTTOV-11.2 with the forecast (*t+24*). *H24.BT_RTTOV[IR3.9,WV6.2, WV7.3, IR10.8, IR8.7, IR9.7, IR12.0, IR13.4]*.
- ***AHI BT_RTTOV(10) from NWPHyb(t+00)***: Synthetic BTs calculated using the RTTOV-11.2 with the analysis (*t+00*). *H00.BT_RTTOV[IR3.9,WV6.2, WV6.9, WV7.3, IR8.6, IR9.6, IR10.3, IR11.2, IR12.3, IR13.3]*.
- ***AHI BT_RTTOV(10) from NWPHyb(t+12)***: Synthetic BTs calculated using the RTTOV-11.2 with the forecast (*t+12*). *H12.BT_RTTOV[IR3.9,WV6.2, WV6.9, WV7.3, IR8.6, IR9.6, IR10.3, IR11.2, IR12.3, IR13.3]*.
- ***AHI BT_RTTOV(10) from NWPHyb(t+24)***: Synthetic BTs calculated using the RTTOV-11.2 with the forecast (*t+24*). *H24.BT_RTTOV[IR3.9,WV6.2, WV6.9, WV7.3, IR8.6, IR9.6, IR10.3, IR11.2, IR12.3, IR13.3]*.
- ***Same for ABI RTTOV BTs.***
- ***Same in future for MTG-FCI or MTG-IRS or IASI***

These basic validation and training datasets have been used for several tasks. One of them consisting of splitting the records in the global dataset into records to generate the validation datasets (1 out 3 positions with offset 0) and the training ones (1 out 3 positions with offset 1). All the 2018 version of GEO-iSHAI coefficients have been calculated with this dataset. For the GEO-iSHAI the changes with respect to GEO-iSHAi v2016 in the coefficients files are the following:

- ***New FG non-linear regression coefficients***: 200.000 profiles (half sea pixels and half land pixels) has been extracted from year 2017 training dataset with a random process in which the probability to be extracted to this reduced training dataset increases with the inverse to the frequency in the histogram of TPW. This reduced dataset with more uniform representativeness of profiles with different precipitable water have been used to train the hybrid FG regressions. The FG regressions coefficient file contains 76 regression

coefficients for different local zenith angles ranging from 0 to 75 degrees and for every atmospheric parameter (54 for temperature profile, 54 for humidity profile and 1 for skin temperature). See GEO-iSHAI ATBD [RD.3] for details on the fields used in the FG regressions. It has been generated FG regression coefficients for SEVIRI, AHI and ABI.

- ***New inverse of covariance matrix of the background error*** $\mathbf{B^{-1}}$: the covariance matrix of the background error between *t+12* and *t+00* ECMWF profiles has been calculated using NWP-Hyb dataset from the 2017 year records. Thus, the B^{-1} matrix is based on ECMWF hybrid profiles from the whole MSG disk.
- ***New EOF file***: the eigenvectors and eigenvalues of the previous 2017 B^{-1} matrix have been used to build the new EOF matrix. In order to use just 7 EOFs and to have 3 for temperature and 3 log(q) profiles plus 1 EOF for SKT, it has been identifies and change the order in the EOFS to have first the 3 main EOFs related to the T profile, then the 3 main EOFs related to the log(q) profile and then the 1 for SKT. Thus, this new EOFs file is based on year 2017 ECMWF hybrid profiles of the training dataset.
- ***New inverse of matrix measurement error*** $\mathbf{E^{-1}}$: the sea pixels of the 2017 year PGE13 training dataset are used to calculate the (BT_{SEVIRI} –BT_{RTTOV}) matrix for channels [*WV6.2, WV7.3, IR10.8, IR12.0, IR13.4*]. Then, the diagonal of this matrix is retained and its inverse is calculated. The E^{-1} matrix is important since it controls the rate of conversion from (BT_{SEVIRI} –BT_{RTTOV}) values to modifications on the (T, log(q)) profiles. For convenience in GEO-iSHAI algorithm (see section 2.2.6 of [RD-3]), the values in the E^{-1} files are the square root.

To avoid some issues (as SEVIRI BT biases, emissivity, contamination by clouds, need of screening in the selection of the records, etc.) and to make the document more readable, the assessment of the performances for these new GEO-iSHAI coefficients files is shown first when GEO-iSHAI uses as input synthetic RTTOV brightness temperatures from ECMWF hybrid analysis (*t+00*) profiles; this experiment is denoted hereafter as **BT_RTTOV case**. Then, the performances are compared with the ones using as input to GEO-iSHAI real bias corrected SEVIRI BTs; this experiment is denoted hereafter as **BT_SEVIRI case**.

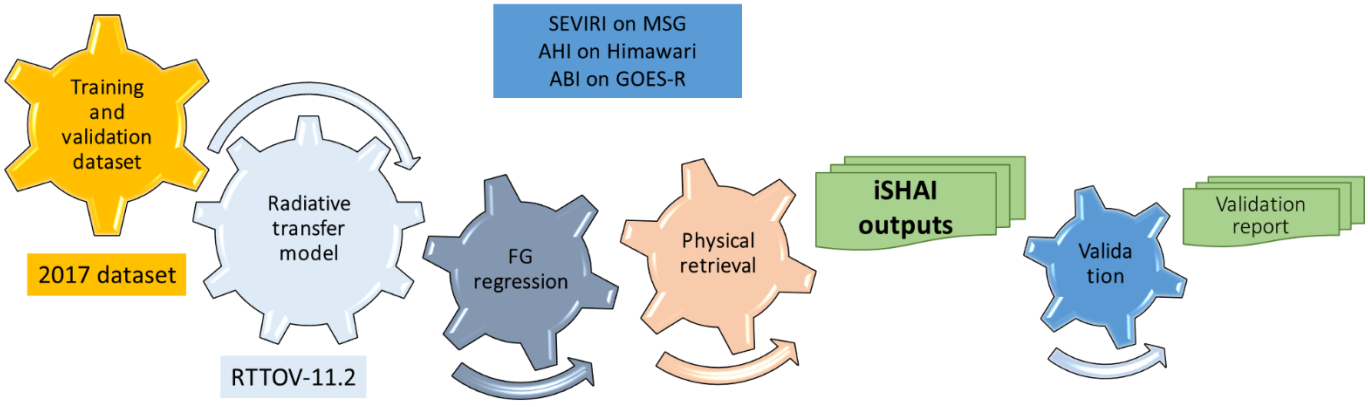

Figure 3: GEO iSHAI validation scheme.

3. VALIDATION RESULTS WITH SEVIRI

Results presented in this section are organised as follows. In Section 3.1, the analysis of the error between the SEVIRI BTs and the synthetic RTTOV BTs at the different steps of the algorithm is first discussed. In section 3.2 an analysis of the vertical performance of the algorithm is made. In section 3.3 the analysis of 2D histograms is made. In Section 3.4 the analysis of spatial validation results are presented. In Section 3.5 the statistical values for LPW, TPW and stability indices are summarized in tables. In Section 3.6 and in Section 3.7 the statistical values for TOZ and SKT are shown respectively.

In all cases the figures and statistical performance are shown from the validation of analysis *t+00* versus *t+24* forecast. The reason to show the performance of t+*24* instead of the performance of *t+12* is that with the improvement of the ECMWF model from 2013 year to 2017 year the separation of lines in rmse profiles and the difference in colour for spatial figures were narrower than in previous validation report ([RD.5]). The performance of analysis *t+00* versus *t+12* forecast is available and could be asked to mmartinezr@aemet.es.

In all the figures and statistical performance the validation dataset used is the dataset 1 out 3 positions with offset 1 of the 2017 year.

In order to assess the performance of iSHAI algorithm it has been made three main validation tests:

1. **Synthetic RTTOV BTs** calculated using as input to RTTOV the ECMWF analysis *t+00* profiles are used as input to the GEO iSHAI and it is denoted hereafter as ***BT_RTTOV case***. It is used to draw the main characteristics of iSHAI and to estimate the potential performance. In this synthetic case the main advantage is that the analysis (*t+00* forecast) can be considered as a real truth and the calculated statistical parameters can be used to assess the statistical performance of iSHAI.
2. **Real bias corrected SEVIRI BTs** are used as input to the GEO iSHAI and it is denoted hereafter as ***BT_SEVIRI case***. It is used to show the deviation from the theoretical one in operational conditions; the calculated statistical parameters in this case has the disadvantage to have no real truth. Thus, the difference in the fields with RTTOV case are due to noise in satellite, errors in RTTOV and errors in iSHAI coefficients in one hand and the lack of a real truth to compare in another. As an example, the source of the differences on the SKT over land field in *BT_SEVIRI case* compared with the one in *BT_RTTOV case* are due to the fact that real SKT is not well represented by ECWMF analysis SKT (there is no truth) and second the errors introduced by iSHAI con SKT estimation due to the errors mentioned above.
3. **Real SEVIRI BTs without bias BT correction** are used as input to the GEO iSHAI and it is denoted hereafter as ***BT_SEVIRI_unc case***. It is used internally to assess the stability of iSHAI algorithm and to advice users on the limitations of the algorithm. The results are not shown here.

3.1 DISTANCE BETWEEN SEVIRI AND SYNTHETIC BTS AT DIFFERENT STEPS

In order to check the added value of the successive steps of the GEO iSHAI algorithm, an inspection of the difference between the synthetic RTTOV BTs calculated using the profiles from the ECMWF analysis (*t+00*) and used here as true profiles, versus the real bias corrected SEVIRI BTs and the synthetic RTTOV BTs at the different steps of the GEO iSHAI algorithm is made first. This inspection has been divided in two parts. First, a spatial analysis of the BT differences is made and later an analysis of the histogram of the BT error is done.

In this subsection, two parameters are checked. The first parameter is the distance between synthetic BTs obtained from profiles from the GEO iSHAI physical retrieval step and real BTs in all SEVIRI channels (IR10.8, IR12.0, WV6.2, WV7.3 and IR13.4). This is denoted as `BT_distance`. The second one, `BT_RMS`, is the same statistics as before, but calculated using non-window channels, i.e. the distance between BTs calculated from WV6.2, WV7.3 and IR13.4 channels.

Before the generation of the figures and the statistical results on this report, an outliers screening method has been implemented. In the screening we are masking as outliers the 2% of the pixels with the largest BT_RMS and BT_distance for every used dataset in this report. That means that we are masking as outliers and removing in all the comparisons and statistical estimations 2% of pixels with the largest BT_RMS and BT_distance for any of the *t+00*, *t+12*, *t+24*, FG and Phy datasets and for the all the cases (SEVIRI RTTOV, SEVIRI and SEVIRI_unc). The Figures without the screening are not shown in this report. In order to use the same set of pixels, the same combined outlier mask has been used for all the Figures and statistical parameter shown in Sections 3 and 4.

In Figure 4, real bias corrected SEVIRI BTs are used as input to the GEO iSHAI and it is denoted as BT_SEVIRI case. The spatial distribution of the mean BT_distance and mean BT_RMS are shown at the three main steps on the GEO iSHAI algorithm. In BT_SEVIRI case, **H24** step means that to calculate BT_distance and BT_RMS real bias corrected SEVIRI BTs and synthetic BTs calculated from the ECMWF forecast *t+24* BTs have been used. **FG** step means that to calculate BT_distance and BT_RMS real bias corrected SEVIRI BTs and profiles after FG regression step have been used. **PHY** step means that to calculate BT_distance and BT_RMS real bias corrected SEVIRI BTs and profiles after FG step and physical retrieval step have been used.

It can be seen in Figure 4 that the FG regression and the physical retrieval steps significantly reduces both BT_distance and BT_RMS. That means that non-linear regression and physical retrieval effectively modify the profiles in correct direction to get a convergence of synthetic and real BTs. The regions with largest errors and residuals are located over land areas.

Figure 5 is similar to Figure 4, but in Figure 5 synthetic RTTOV BTs from the ECMWF analysis (*t+00*) (BT_RTTOV case) are used as input to the GEO iSHAI module (instead of real bias corrected SEVIRI BTs). It can be seen that the GEO iSHAI in Figure 5 has similar behaviour than in Figure 4 but without the regions with large errors that appear in BT_SEVIRI case (when real bias corrected SEVIRI BTs are the input).

The larger residuals on Figure 5 compared to Figure 4 are associated to several issues, such as uncertainties on emissivity fields, contamination with clouds on some pixels (not well filtered by Cloud Mask), errors in the radiative transfer model RTTOV, noise of real SEVIRI image, lack of a real truth (SKT from ECMWF analysis is used as proxy), etc. On Figure 4, the largest values of BT_distance are also likely due to errors between SEVIRI BT at window channels and the ones calculated from ECMWF analysis due to the fact that skin temperature on ECMWF analysis does not represent real skin temperature over desert regions, mountains, etc.

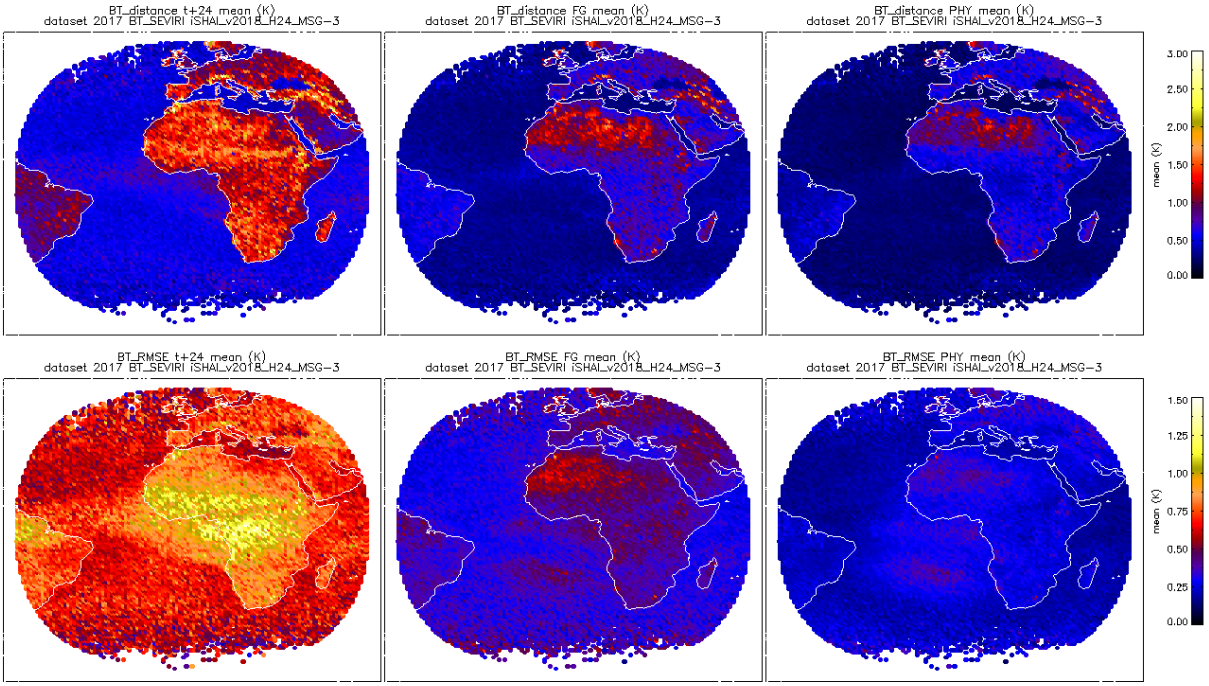

Figure 4: ***BT_SEVIRI case:*** *Spatial distribution of mean BT_distance (top) and BT_RMS (bottom) between real bias corrected SEVIRI BTs and ECMWF analysis synthetic BTs at different steps of GEO iSHAI. Left) forecast t+24 synthetic BTs, middle) synthetic BTs after FG step and right) using RTTOV BTs after FG+physical retrieval steps.*

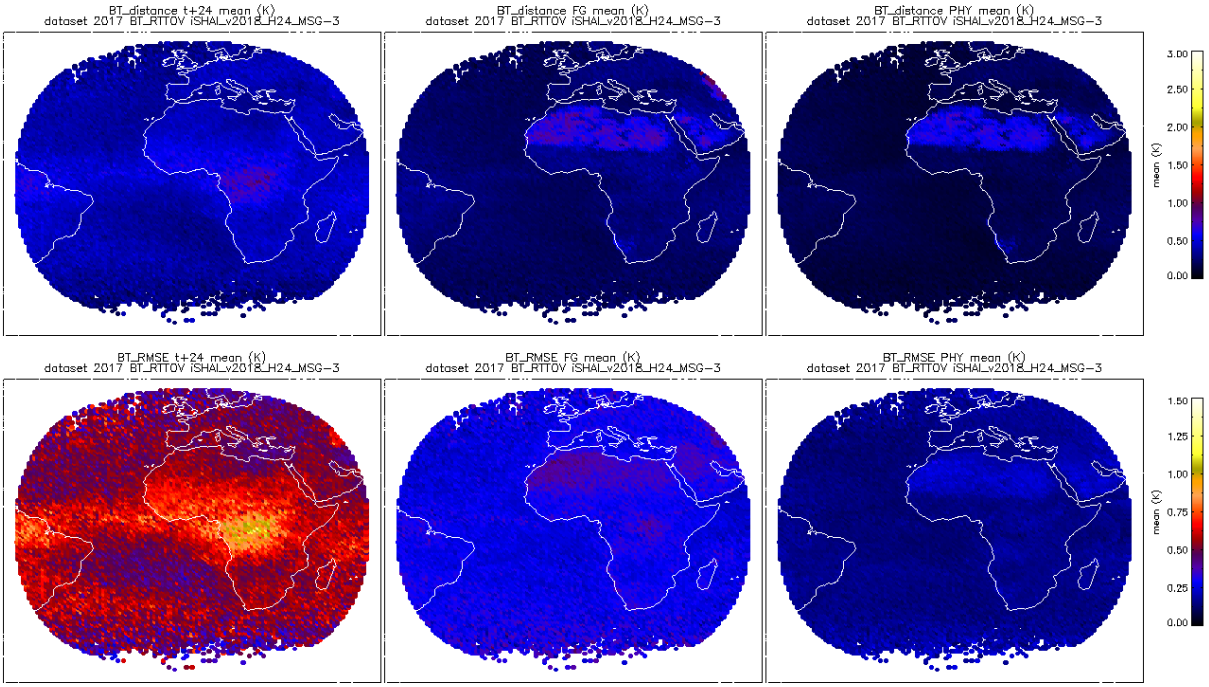

Figure 5: ***BT_RTTOV case:*** *Same that Fig. 4 but synthetic RTTOV BTs from ECMWF analysis are used as input to GEO iSHAI. Spatial distribution of mean BT_distance (top) and BT_RMS (bottom) between synthetic BTs from ECMWF (t+00) and synthetic BTs at different step of GEO iSHAI. Left) forecast t+24 synthetic BTs, middle) synthetic BTs after FG step and right) using RTTOV BTs after FG+physical retrieval steps.*

It can be seen in Figure 4 and 5 that the FG regression and the physical retrieval steps significantly reduces both `BT_distance` and `BT_RMS`. As conclusion of the analysis of Figures 4 and 5, the physical retrieval algorithm implemented in the GEO iSHAI algorithm works fine and the retrieved

(T, q) profiles reduces significantly the distance between the bias corrected SEVIRI BTs and the synthetic RTTOV BTs.

On the other hand, the analysis of GEO iSHAI algorithm steps with synthetic RTTOV as input can be representative of the performance of the GEO iSHAI algorithm avoiding the issues related to real measurements mentioned in the previous paragraph. For these reasons, and to avoid the need of additional screening filters, especially hard to make over land, the validation on the next sections is made always showing first the statistical values from the synthetic BT_RTTOV case.

Not shown here, similar figures using real uncorrected bias SEVIRI BTs have been calculated; the performance in the case of real uncorrected bias BT is worse than the performance in the case of real bias corrected BTs; this, in fact, is another justification on the need of a good and updated BT bias correction.

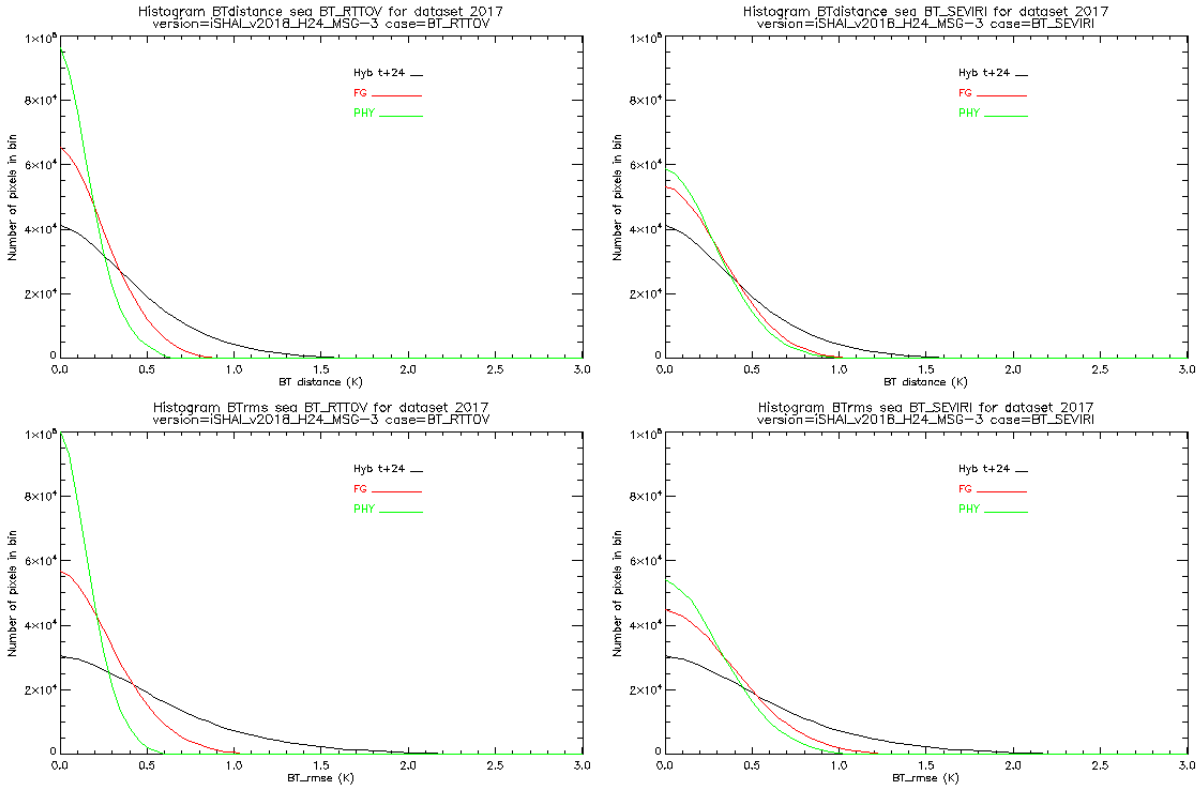

Figure 6: Histogram of top) `BT_distance` *(distance in IR10.8, IR12.0, WV6.2, WV7.3 and IR13.4channels) and bottom)* `BT_RMS` *(distance in absorption channels) at different steps of the GEO iSHAI. Left) BT_RTTOV case, right) BT_SEVIRI case.*

The histograms with `BT_distance` and with `BT_RMS` for the BT_RTTOV case and the BT_SEVIRI case at the different steps of the GEO iSHAI module are shown in Figure 6. It can be seen that the FG+physical retrieval steps reduces significantly the number of profiles with `BT_distance` and `BT_RMS` greater than 0.6. Also, just the FG step reduces both `BT_distance` and `BT_RMS`. The `BT_RMS` has been verified because in the GEO iSHAI code if the `BT_RMS` in the pixel is greater than a threshold, then the physical retrieval module is applied. The analysis of the histograms of the error and `BT_RMS` can be used to select the optimal values for the configurable parameters `BT_RMS_THRESHOLD` and `MAX_RESIDUAL` (these parameters are read from the ASCII GEO-iSHAI configuration file and an explanation of the impact in the selection in these parameters can be found in the User Manual [RD-4]).

3.2 ANALYSIS OF THE PERFORMANCE AT DIFFERENT VERTICAL LEVELS

In Figure 7, the RMSEs between the q profiles after several steps in the GEO iSHAI for the full disc dataset at the 54 RTTOV levels have been represented.

The profiles of the ECMWF analysis (*t+00*) from NWP-Hyb datasets (137 hybrid levels interpolated to the 54 RTTOV level) have been considered as the truth.

The statistical values for the specific humidity at mid-levels show better performance for the FG regression and the FG+physical retrieval steps than the background NWP model (ECMWF GRIB files on hybrid levels from *t+24* forecast). This is likely due to the added value of the WV SEVIRI channels, the reduction in the RMSE at these levels indicates that the GEO iSHAI slightly improves the q profile from background NWP.

The performance is better over sea pixels. The worse performance over land can be due to a combination of all sources of errors that can affect the calculation of the synthetic BT (uncertainties in the emissivity atlas, errors due to contamination with clouds on some pixels (not well filtered by the Cloud Mask), errors in the radiative transfer model RTTOV, noise of real SEVIRI image, etc.)

Several experiments, not shown here, to compare the GEO iSHAI performance have been made. The first experiment is to suppress the FG regression step and use directly as First Guess the *t+24* forecast profiles from ECMWF GRIB files on hybrid levels; but the performance of GEO iSHAI with FG regression step is slightly better.

These experiments and the faster executions of GEO iSHAI with FG regression step (avoiding the execution of the physical retrieval step on all clear FOR) have inclined us to maintain the FG regression step on the GEO iSHAI algorithm. Hereafter, in the figures the meaning of the labels is the following:

1. ***Hybrid t+24***: indicates that the value has been calculated using the comparison of ECMWF *t+24* forecast and the ECMWF analysis *t+00* as truth.
2. **FG**: indicates that the value has been calculated using comparison of the result to execute the non-linear regressions of FG step over the satellite BTs case and the ECMWF *t+24* forecast and the ECMWF analysis *t+00* as truth.
3. **PHY**: indicates that the value has been calculated using comparison of the result to execute the non-linear regressions of FG step followed by the physical retrieval step over the satellite BTs case and the ECMWF *t+24* forecast and the ECMWF analysis *t+00* as truth.

It can be seen in 2012 Validation Reports [RD.1] that the use of ECMWF with 15 fixed pressure levels profiles as input to the PGE13 SPhR created several “peaks” and irregularities in the RMSE and bias vertical distribution centred at the 15 fixed pressure levels. The comparison of Figure 7 of this report with Figure 11 of the 2012 Validation Report [RD.1] is another reason to strongly recommend the use of GRIB files with the maximum number of vertical levels as possible as the background NWP input to GEO iSHAI. For this reason the performance of GEO iSHAI processor with GRIB files on hybrid levels as background NWP input is the best possible.

The NWC/GEO package version 2018 will continue with the use of the fixed pressure levels as background NWP input to GEO iSHAI, since the current version and the 2018 version of NWC SAF library only allows reading GRIB files on fixed pressure. GEO-iSHAI is just one advance of future versions of NWC/GEO processing. The details to activate GEO-iSHAI on hybrid levels instead to the regular GEO iSHAI on P levels can be found in the GEO-iSHAI User Manual [RD.4].

In order to show that the source of the increase of q rmse on land SEVIRI case is associated to the high q rmse error in tropical forest at Equatorial region (see Figure 15 in section 3.4), in Figure 8 the profiles of q rmse but just for European latitude (considered as latitude greater than 36 ºN) are shown. It can be seen the strong reduction in q rmse in the land SEVIRI case in the layer 900-600 hPa.

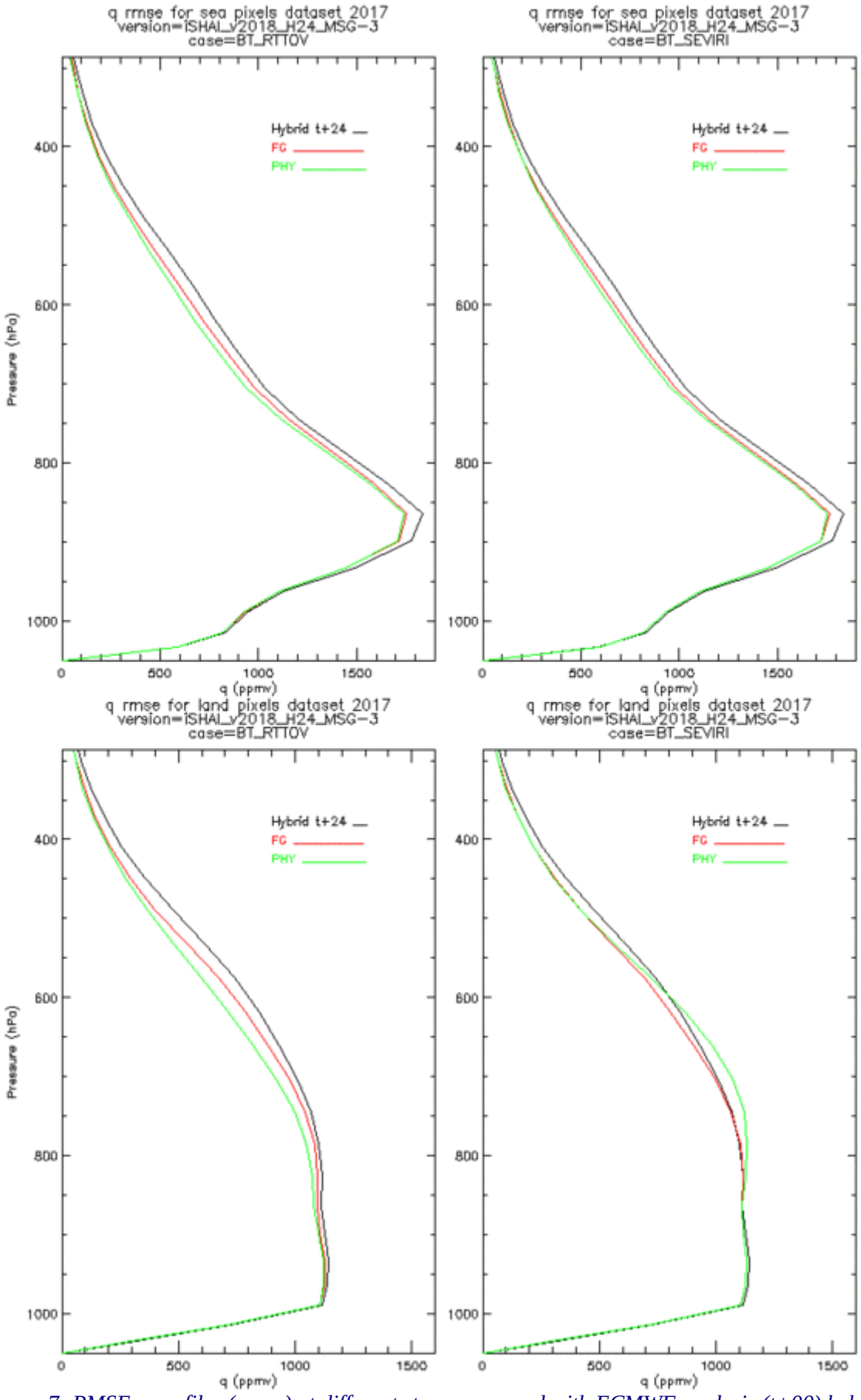

Figure 7: RMSE q profiles (ppmv) at different steps compared with ECMWF analysis (t+00) hybrid profiles. Left) BT_RTTOV case, right) BT_SEVIRI case. Top) RMSE of q over sea pixels, bottom) RMSE of q over land pixels.

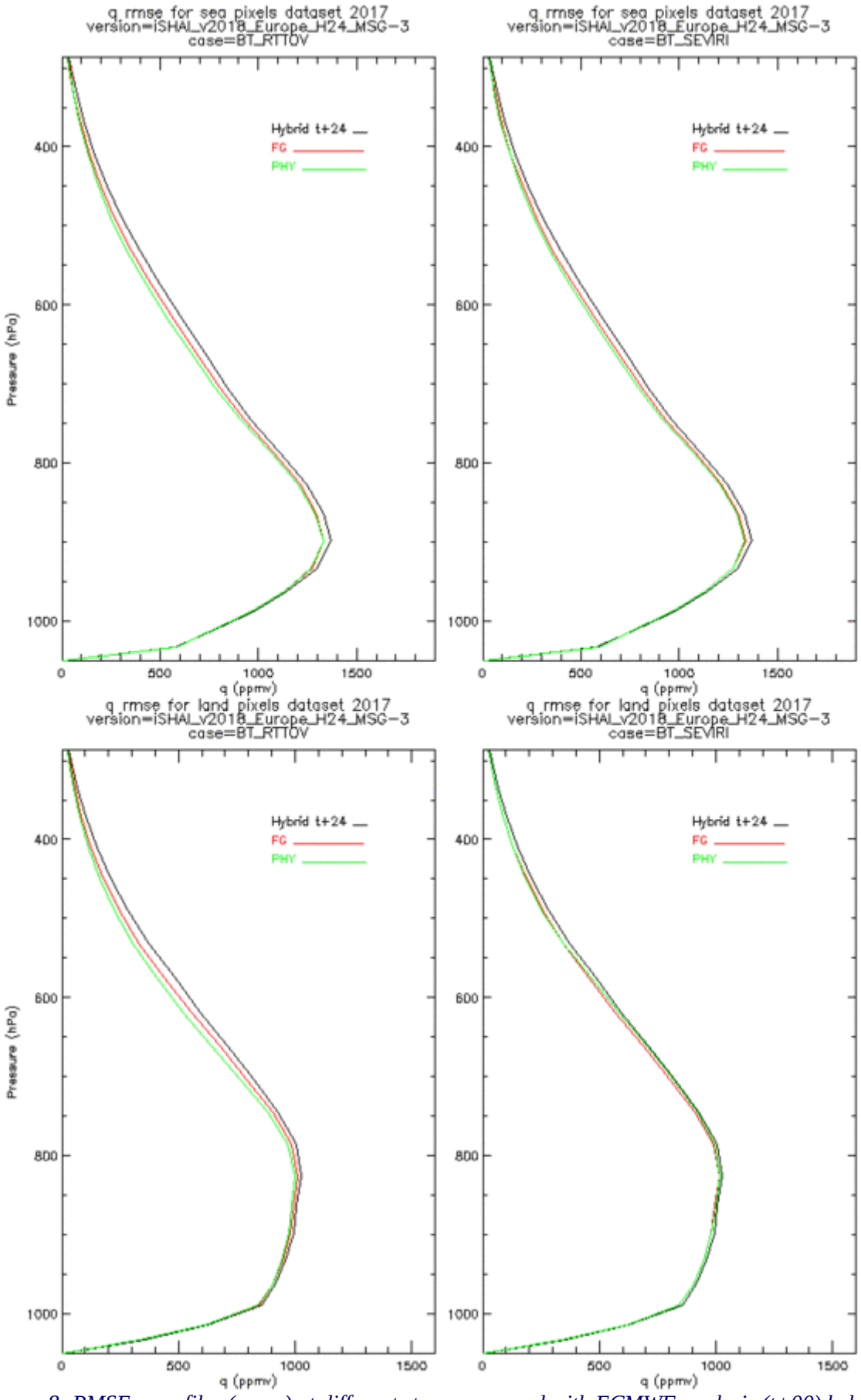

Figure 8: RMSE q profiles (ppmv) at different steps compared with ECMWF analysis (t+00) hybrid profiles . Left) BT_RTTOV case, right) BT_SEVIRI case. Top) RMSE of q over sea pixels, bottom) RMSE of q over land pixels. On pixels with latitude greater than 36º N

3.3 2D DIMENSIONAL HISTOGRAMS OF GEO iSHAI PARAMETERS

To avoid multiplying the number of Figures, only the two dimensional histograms for each one of the LPW and TPW parameters calculated from the retrieved profiles at different steps are presented here. It has been used always as truth the ECMWF analysis denoted here as NWP-Hyb (*t+00*) profiles. In Figure 9 for sea pixels and in Figure 10 for land pixels for BT_RTTOV case. Same Figures but for BT_SEVIRI case can be seen in Figures 11 and 12. The statistical values (RMSE, bias and correlation) that appear in the 2D histograms are also written at the end of this report in the tables of the Section 3.5 for a more comfortable read and comparison.

Note that GEO-iSHAI BL is the precipitable water in a layer between P_{sfc} to 850 hPa. GEO-iSHAI ML is the precipitable water in a layer between 850 hPa to 500 hPa. GEO iSHAI HL is the precipitable water in a layer between 500 hPa to 0.1 hPa. GEO iSHAI TPW is the total precipitable water i.e the precipitable water in a layer between P_{sfc} to 0.1 hPa.

It can be seen in Figures 9 to 12 that statistical values of the GEO-iSHAI parameters reproduce the performance suggested by the vertical analysis from Figure 7 and 8. The parameters with the largest added value are ML and HL parameters; this fact is due to the WV channels.

Other important result is that the 2D histograms of the GEO-iSHAI parameters show no significant bias and it is not needed any post processing correction.

In the case of BT_SEVIRI case over land some spread in the 2D histograms shows up; the cause of this spread could be due to the factors mentioned before (cloud contaminated pixels, uncertainties in the emissivity atlases, disagreements in the skin temperature from the ECMWF, etc). From the comparison ML 2D histograms over of Figures 12 on the full disc and Figure 33 on Europe region it can be seen the spread up in Figure 12 is caused mainly by the tropical forest at Equatorial regions.

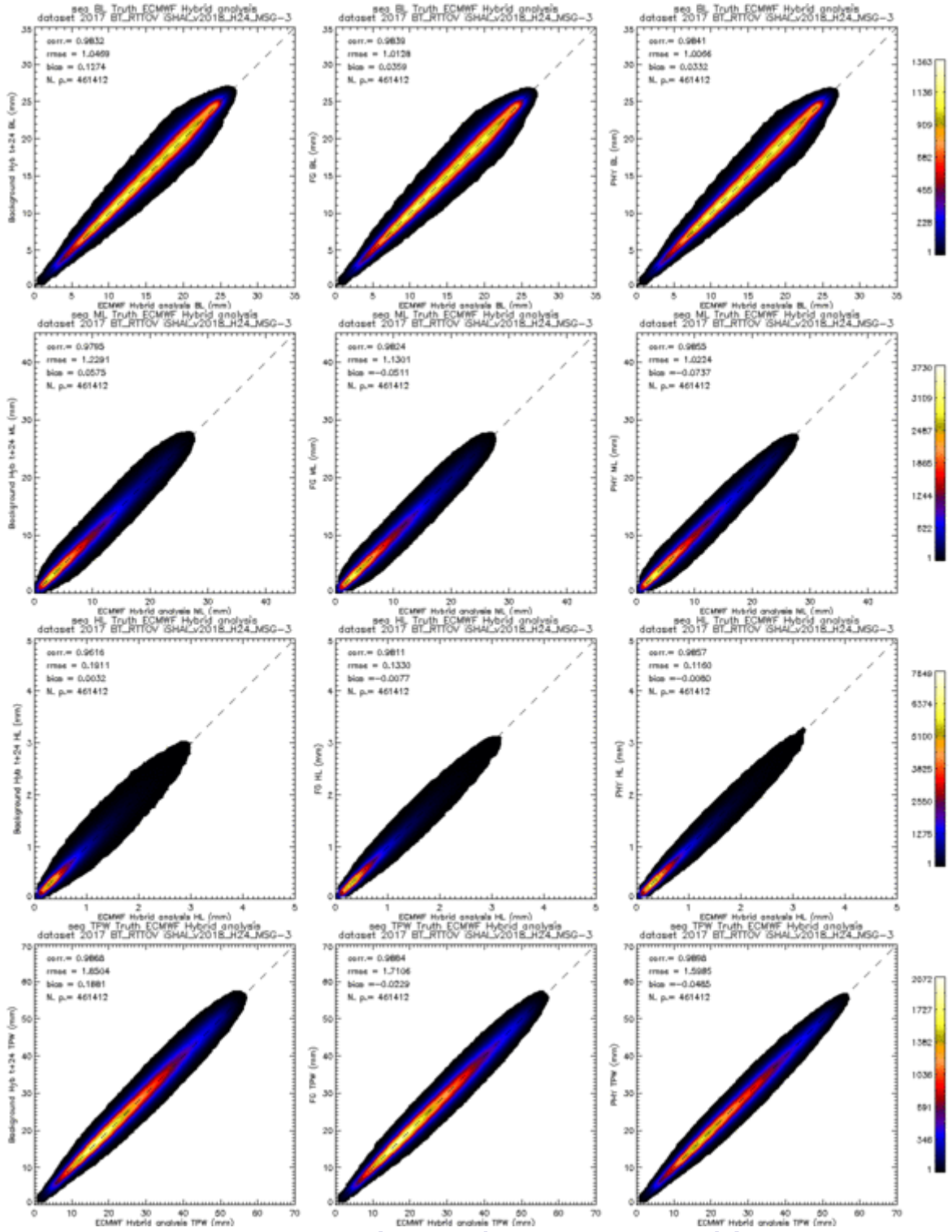

*Figure 9: **BT_RTTOV** case: LPW and TPW 2D histograms over **sea** validation points. From top to bottom BL, ML, HL and TPW parameters. Left) BL, ML, HL and TPW parameters calculated directly from background ECMWF from hybrid profiles from (t+24) forecast, centre) BL, ML, HL and TPW parameters calculated after FG step profile using as input BT_RTTOV (t+00), right) BL, ML, HL and TPW parameters calculated after physical retrieval step profile. In all case the ground truth are the BL, ML, HL and TPW calculated from ECMWF analysis (t+00) profiles.*

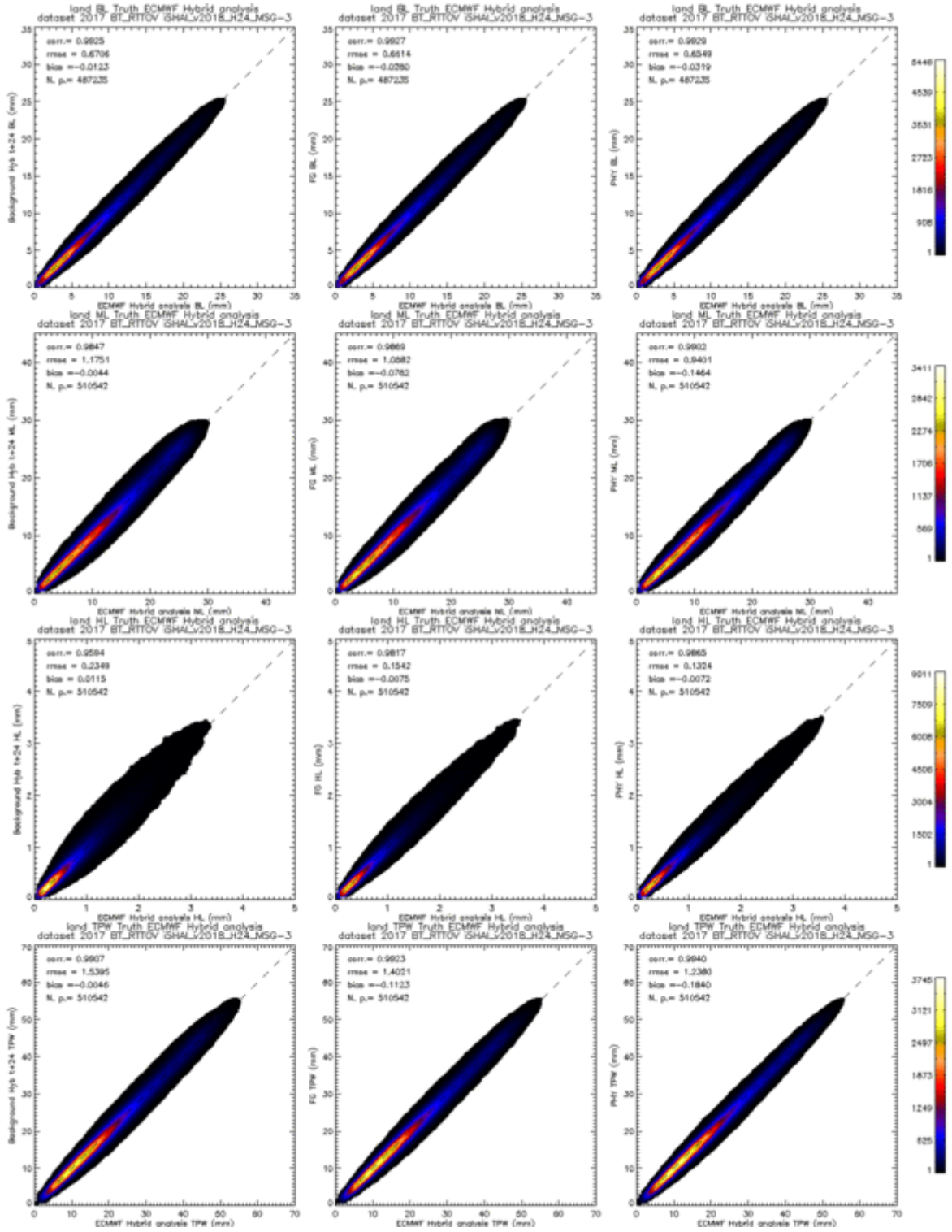

*Figure 10: **BT_RTTOV** case: LPW and TPW 2D histograms over **land** validation points. From top to bottom BL, ML, HL and TPW parameters. Left) BL, ML, HL and TPW parameters calculated directly from background ECMWF from hybrid profiles from (t+24) forecast, centre) BL, ML, HL and TPW parameters calculated after FG step profile using as input BT_RTTOV (t+00), right) BL, ML, HL and TPW parameters calculated after physical retrieval step profile. In all case the ground truth are the BL, ML, HL and TPW calculated from ECMWF analysis (t+00) profiles.*

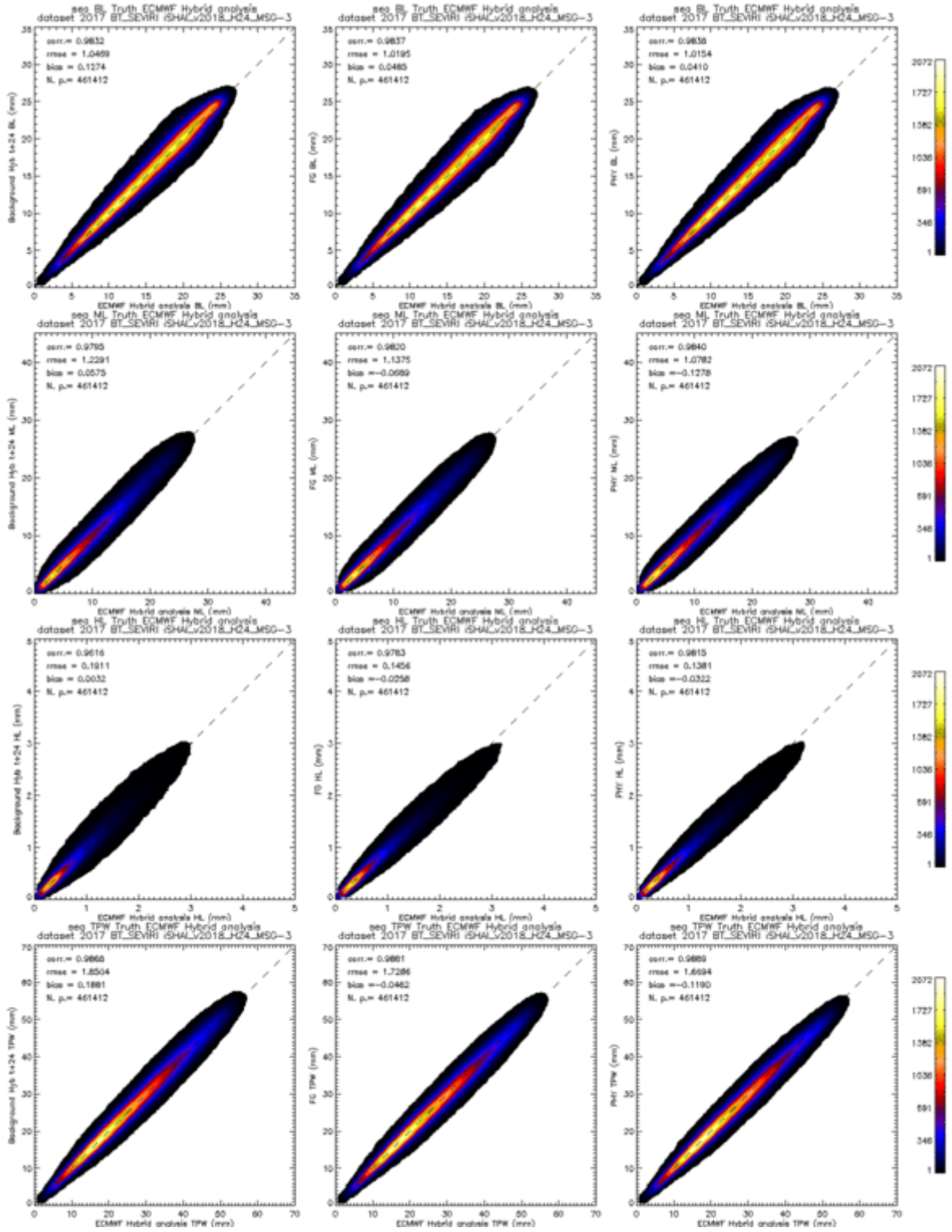

*Figure 11: **BT_SEVIRI** case: LPW and TPW 2D histograms over **sea** validation points. From top to bottom BL, ML, HL and TPW parameters. Left) BL, ML, HL and TPW parameters calculated directly from background ECMWF from hybrid profiles from (t+24) forecast, centre) BL, ML, HL and TPW parameters calculated after FG step profile using as input using real bias corrected SEVIRI BT, right) BL, ML, HL and TPW parameters calculated after physical retrieval step profile. In all case the ground truth are the BL, ML, HL and TPW calculated from Hybrid ECMWF analysis(t+00) profiles.*

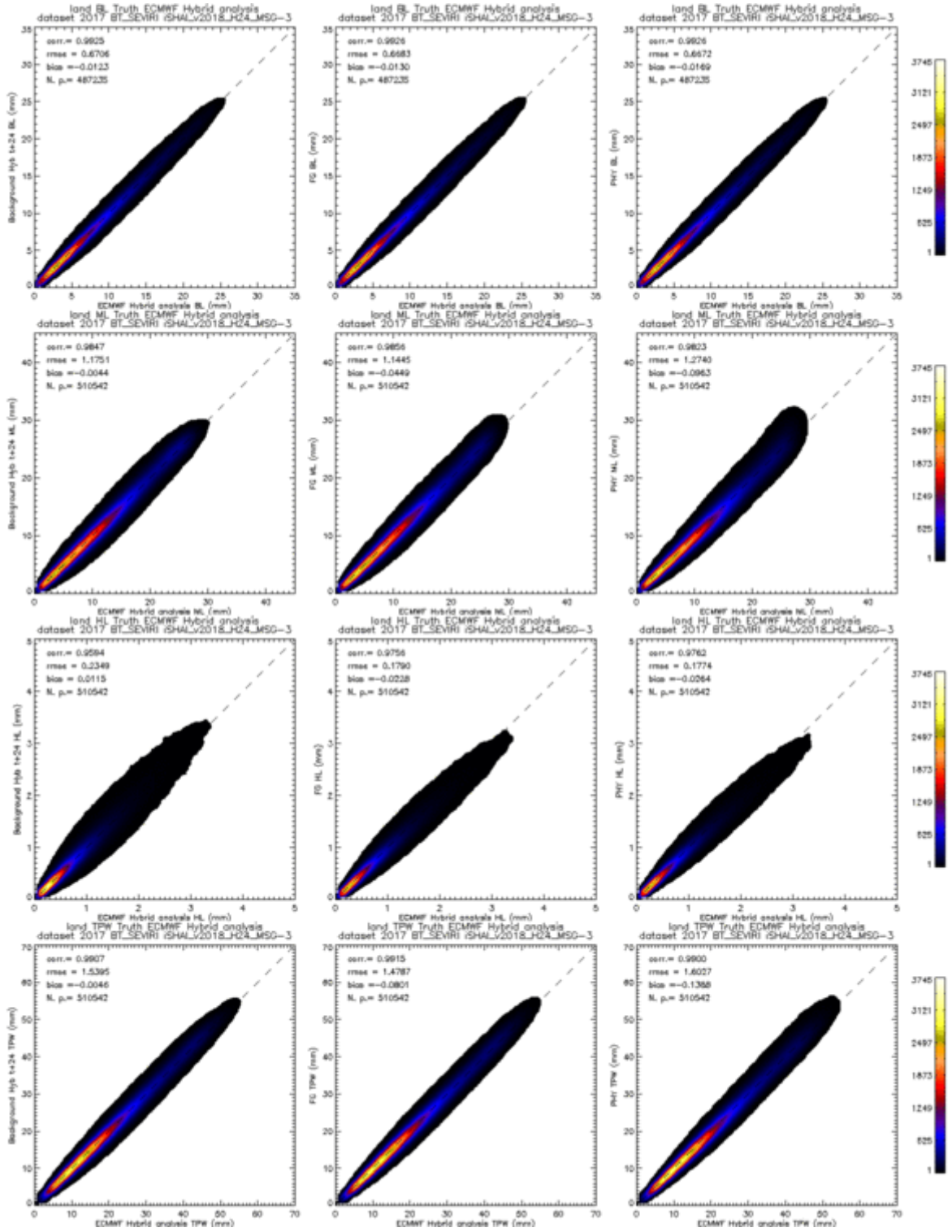

*Figure 12: **BT_SEVIRI** case: LPW and TPW 2D histograms over **land** validation points. From top to bottom BL, ML, HL and TPW parameters. Left) BL, ML, HL and TPW parameters calculated directly from background ECMWF from hybrid profiles from (t+24) forecast, centre) BL, ML, HL and TPW parameters calculated after FG step profile using as input using real bias corrected SEVIRI BT, right) BL, ML, HL and TPW parameters calculated after physical retrieval step profile. In all case the ground truth are the BL, ML, HL and TPW calculated from Hybrid ECMWF analysis (t+00) profiles.*

3.4 SPATIAL ANALYSIS OF GEO iSHAI PARAMETERS

In Figures 13 and 15 the spatial performance of the LPW and TPW parameters for BT_RTTOV case and BT_SEVIRI case respectively are shown.

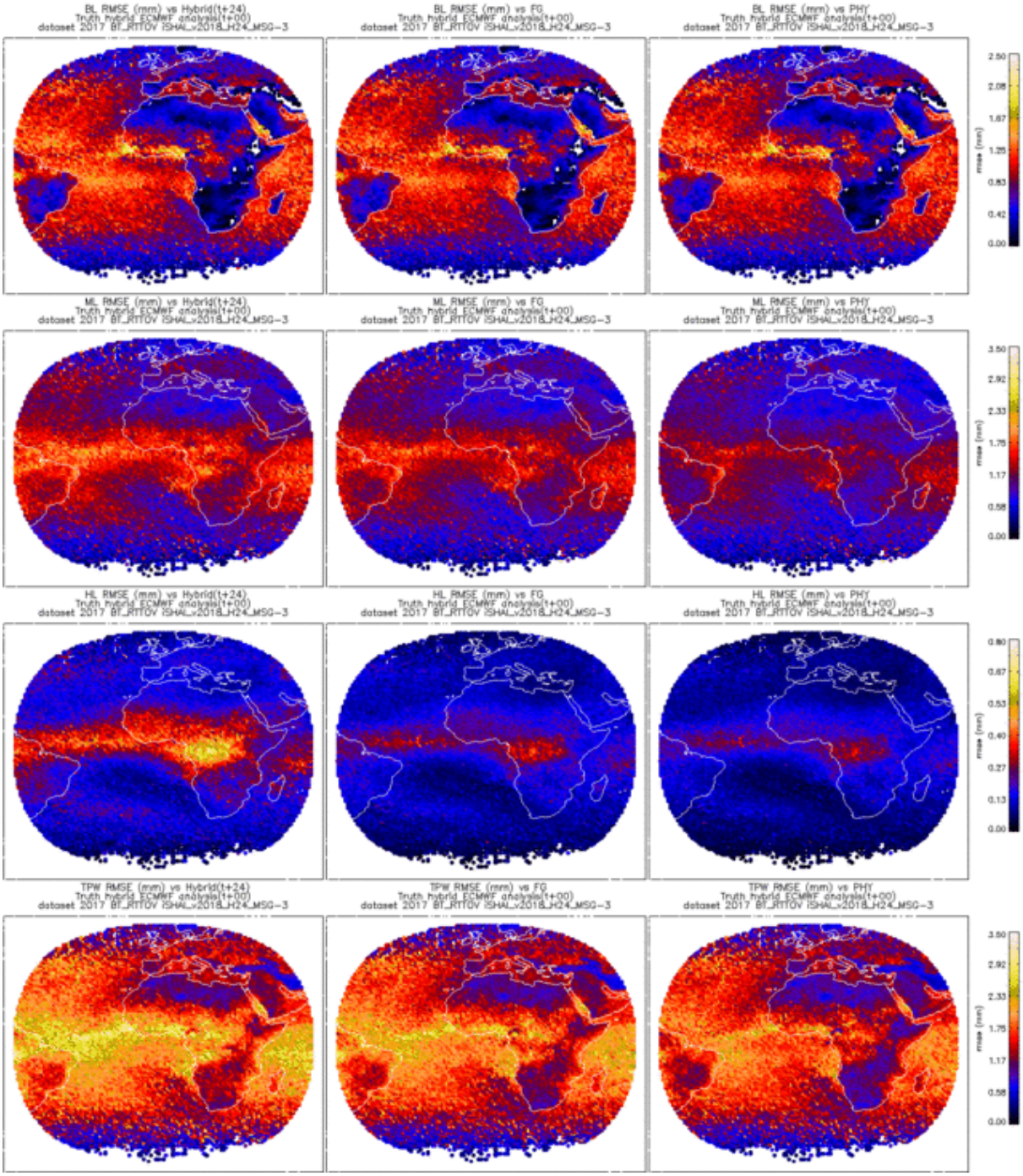

*Figure 13: **BT_RTTOV case:** Spatial distribution of the BL, ML, HL and TPW RMSE over validation points in 2017 dataset. From top to bottom BL, ML, HL and TPW parameters. Left) BL, ML, HL and TPW RMSE calculated directly from background ECMWF hybrid GRIB (t+24), centre) BL, ML, HL and TPW RMSE calculated after FG step profile, right) BL, ML, HL and TPW RMSE calculated after physical retrieval step profile. In all case the ground truth are the BL, ML, HL and TPW calculated from NWP-Hyb ECMWF analysis (t+00) profiles.*

The greatest values of ML and HL RMSE appear near the equatorial belt. But, when the relative ML RMSE are calculated, this effect disappears due to the high amount of precipitable water close to the equatorial belt. This effect can be seen in Figures 14 and 16.

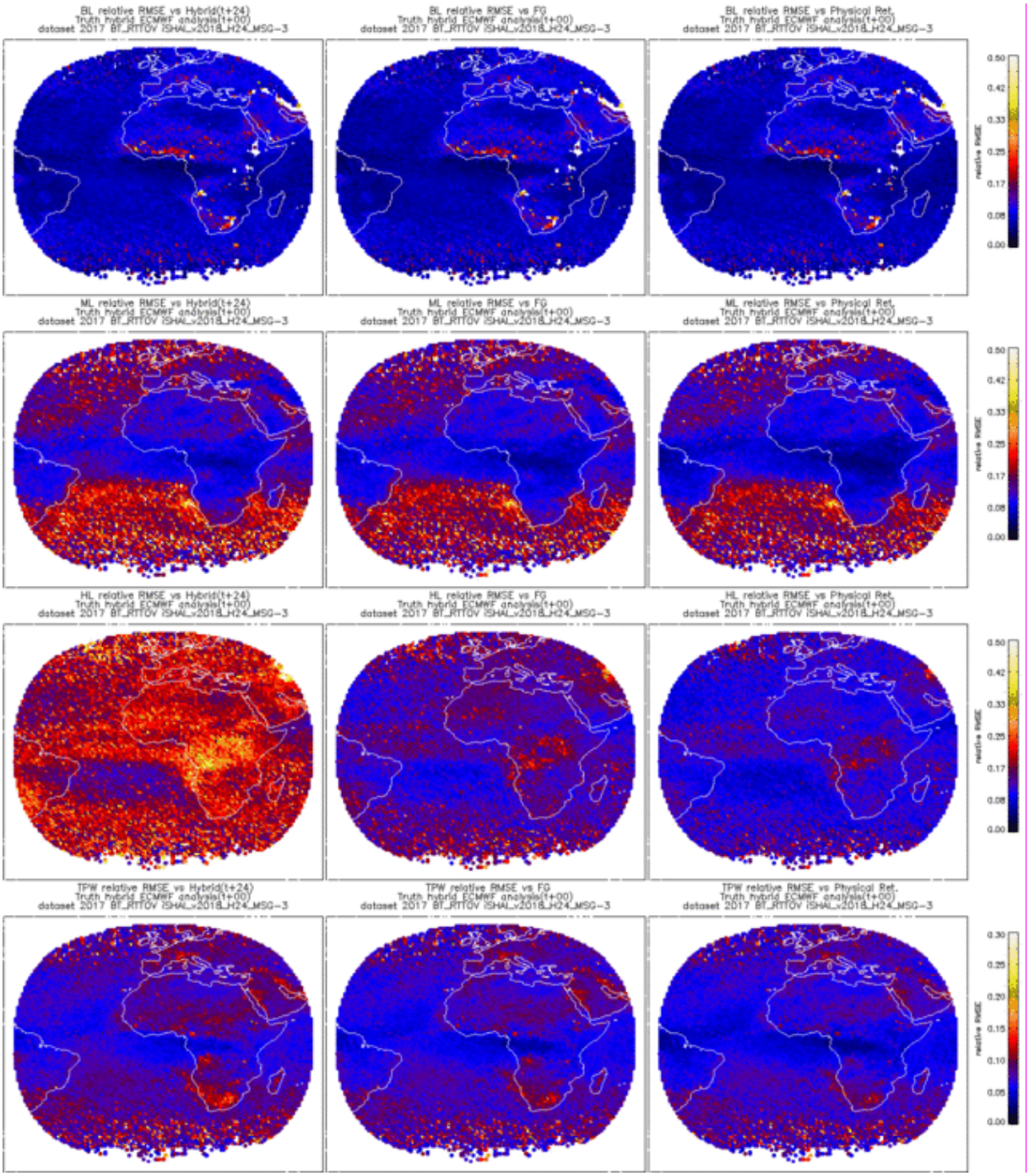

Figure 14: ***BT_RTTOV case:*** *Same that Figure 13 but relative RMSE instead of RMSE.*

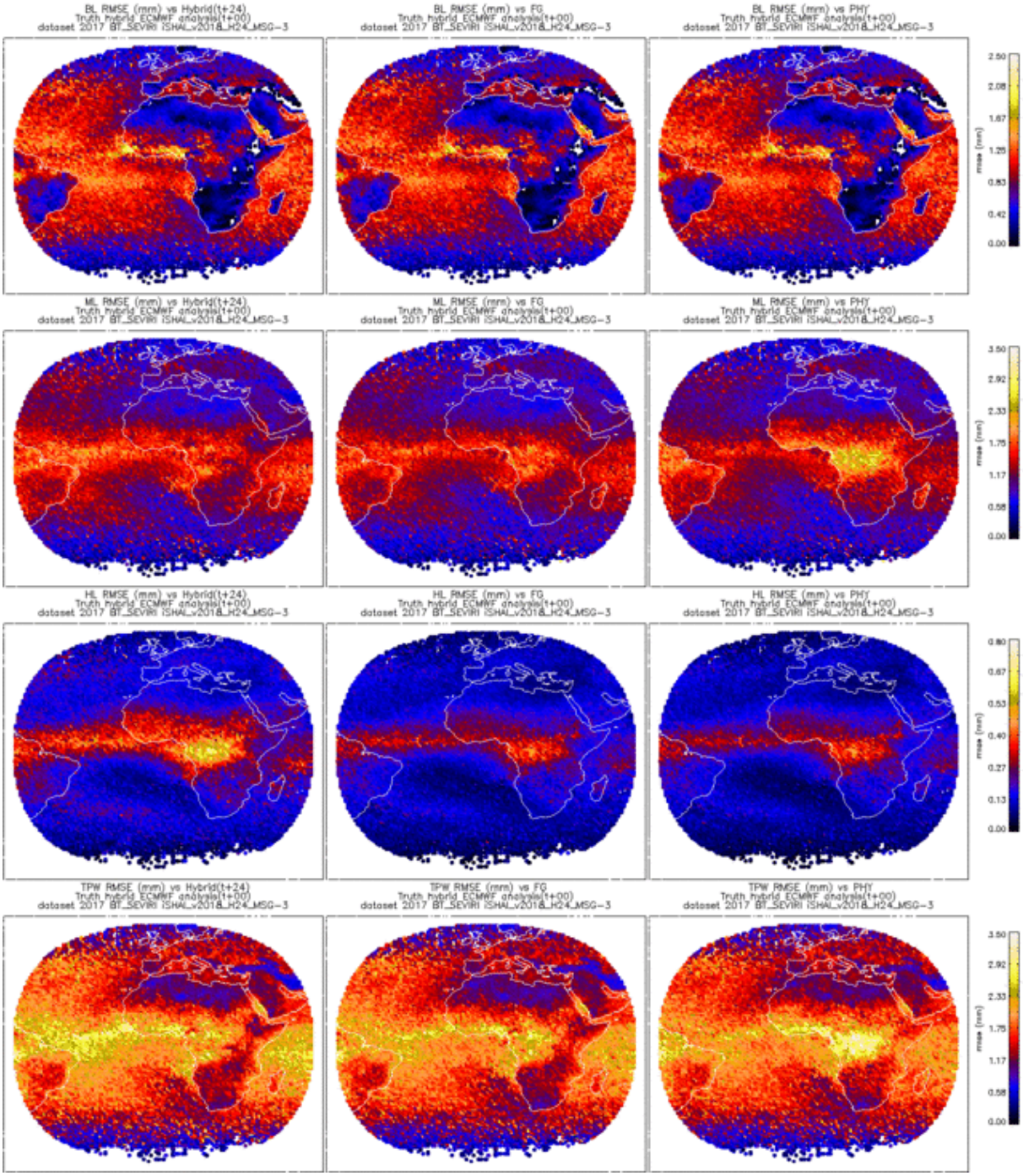

Figure 15: ***BT_SEVIRI case:*** *Spatial distribution of the BL, ML, HL and TPW RMSE over validation points in 2017 dataset. From top to bottom BL, ML, HL and TPW parameters. Left) BL, ML, HL and TPW RMSE calculated directly from background ECMWF hybrid GRIB (t+24), centre) BL, ML, HL and TPW RMSE calculated after FG step profile, right) BL, ML, HL and TPW RMSE calculated after physical retrieval step profile. In all case the ground truth are the BL, ML, HL and TPW calculated from NWPHyb ECMWF analysis(t+00) profiles.*

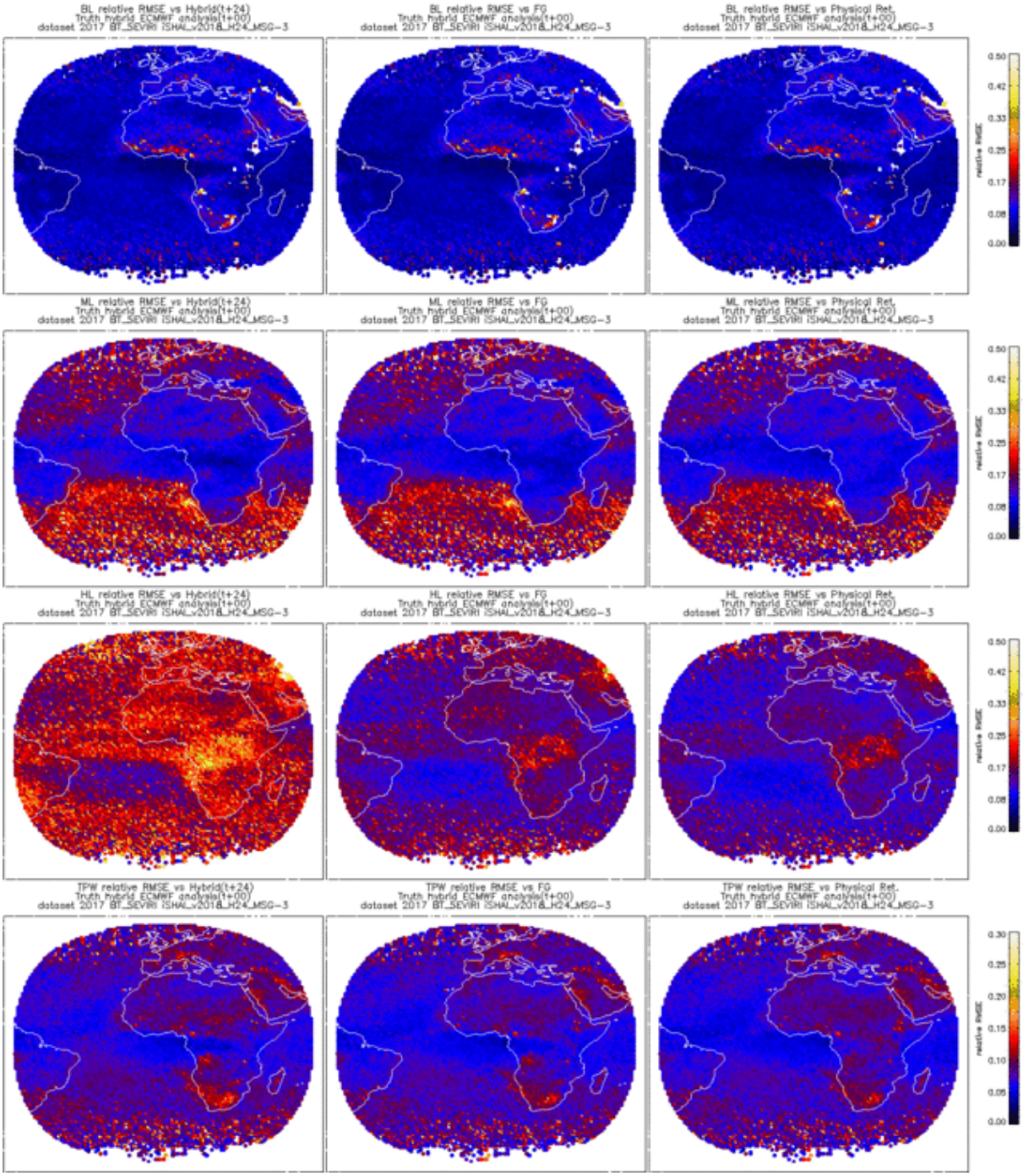

Figure 16: ***BT_SEVIRI case:*** *Same that Figure 15 but relative RMSE instead of RMSE.*

3.5 STATISTICAL SUMMARY OF LPW AND STABILITY INDICES

In order to allow a better comparison, the statistical values that appear inside the 2D histograms have been collected below in Tables 3 to 6.

BL sea	NWPHyb(t+24)	FG	Phy. Retrieval
RMSE (kg/m^2)	1,047	1,013	1,007
BIAS (kg/m^2)	0,127	0,036	0,033
ML sea	NWPHyb(t+24)	FG	Phy. Retrieval
RMSE (kg/m2)	1,229	1,130	1,022
BIAS (kg/m2)	0,058	-0,051	-0,074
HL sea	NWPHyb(t+24)	FG	Phy. Retrieval
RMSE (kg/m2)	0,191	0,133	0,116
BIAS (kg/m2)	0,003	-0,008	-0,008
TPW sea	NWPHyb(t+24)	FG	Phy. Retrieval
RMSE (kg/m2)	1,850	1,711	1,598
BIAS (kg/m2)	0,188	-0,023	-0,048

BL land	NWPHyb(t+24)	FG	Phy. Retrieval
RMSE (kg/m^2)	0,671	0,661	0,655
BIAS (kg/m^2)	-0,012	-0,028	-0,032
ML land	NWPHyb(t+24)	FG	Phy. Retrieval
RMSE (kg/m^2)	1,175	1,088	0,940
BIAS (kg/m2)	-0,004	-0,078	-0,146
HL land	NWPHyb(t+24)	FG	Phy. Retrieval
RMSE (kg/m^2)	0,235	0,154	0,132
BIAS (kg/m2)	0,011	-0,007	-0,007
TPW land	NWPHyb(t+24)	FG	Phy. Retrieval
RMSE (kg/m^2)	1,539	1,402	1,238
BIAS (kg/m2)	-0,005	-0,112	-0,184

*Table 3: **BT_RTTOV case:** Statistical parameters for BL, ML, HL and TPW parameters over the Full Disk validation points in year 2017 dataset. Left) sea pixels, right) land pixels.*

In the case of GEO-iSHAI validation with real bias corrected SEVIRI BTs the performance has the same behaviour but with higher figures and irregular distribution of the RMSE over the land pixels. These irregularities in the figures of the statistical value over land are due to the issues explained in Section 3.1.

ML parameter shows a significant theoretical reduction in RMSE with GEO-iSHAI. From the values of Table 3 for sea pixels in the BT_RTTOV case, it can be seen a reduction in ML RMSE of 8% for FG step and 16% after physical retrieval over sea pixels. The reduction of ML RMSE over land pixels is greater than over sea pixels and it represents a 19% of reduction in the ML RMSE after the physical retrieval step.

After the inspection of Table 4 (BT_SEVIRI case) the values using real bias corrected SEVIRI BT are not so large; but there is still one reduction of the ML RMSE of 7% for FG step and 12% after physical retrieval in sea pixels. It should be remembered that these values have been obtained after the screening to remove the pixels with largest `BT_distance` and `BT_RMS`. If a perfect screening would be possible and a real truth could be obtained, then the performance would tend to the theoretical reduction in RMSE for the BT_RTTOV case. As in the analysis of previous statistical values, the combinations of several sources of errors and uncertainties over land are a potential reason to explain the worse performance of ML over land.

In the case of HL parameter the percentage in the reduction with GEO-iSHAI module are even higher. For HL RMSE in the BT_RTTOV case the theoretical reduction is around 39% over sea pixels and 43% over land pixels after physical retrieval step. In the BT_SEVIRI case the reduction

is 27% over sea pixels and 24% over land pixels. This better performance of HL parameter confirms that the WV channels have the greatest contribution and the source of errors as emissivity uncertainties and skin temperature affect less the HL parameter.

BL sea	NWPHyb(t+24)	FG	Phy. Retrieval
RMSE (kg/m^2)	1,047	1,020	1,015
BIAS (kg/m^2)	0,127	0,049	0,041
ML sea	NWPHyb(t+24)	FG	Phy. Retrieval
RMSE (kg/m2)	1,229	1,138	1,078
BIAS (kg/m2)	0,058	-0,069	-0,128
HL sea	NWPHyb(t+24)	FG	Phy. Retrieval
RMSE (kg/m2)	0,191	0,146	0,138
BIAS (kg/m2)	0,003	-0,026	-0,032
TPW sea	NWPHyb(t+24)	FG	Phy. Retrieval
RMSE (kg/m2)	1,850	1,729	1,669
BIAS (kg/m2)	0,188	-0,046	-0,119

BL land	NWPHyb(t+24)	FG	Phy. Retrieval
RMSE (kg/m^2)	0,671	0,668	0,667
BIAS (kg/m^2)	-0,012	-0,013	-0,017
ML land	NWPHyb(t+24)	FG	Phy. Retrieval
RMSE (kg/m^2)	1,175	1,144	1,274
BIAS (kg/m2)	-0,004	-0,045	-0,096
HL land	NWPHyb(t+24)	FG	Phy. Retrieval
RMSE (kg/m^2)	0,235	0,179	0,177
BIAS (kg/m2)	0,011	-0,023	-0,026
TPW land	NWPHyb(t+24)	FG	Phy. Retrieval
RMSE (kg/m^2)	1,539	1,479	1,603
BIAS (kg/m2)	-0,005	-0,080	-0,139

*Table 4: **BT_SEVIRI case:** Statistical parameters for BL, ML, HL and TPW parameters over the Full Disk validation points in year 2017 for odd pixels dataset. Left) sea pixels, right) land pixels.*

The former confirms the results of the vertical analysis of the performance made in Section 3.2 that showed a reduction in the RMSE and an improvement over the background NWP in the q profile at middle levels. The reduction of RMSE in the middle levels of the q profile is likely the main contribution for the reduction in the TPW RMSE.

In the case of the stability indices, there is not a clear statistical reduction in the RMSE with GEO iSHAI. Looking at Table 5 for the BT_RTTOV case, the performance is better for the stability indices which involve the lower level at 850 hPa (Showalter Index and KI). Likely, this is due to the fact that SEVIRI has limited information to improve the temperature vertical information beyond the forecast. This fact is also explained from the vertical analysis of section 3.2; the highest reduction on q RMSE is on middle and high levels due to WV channels. Thus, it would be advisable to start looking for optimal stability indices from satellite retrievals of temperature and humidity profiles.

But although the statistical validation is not much better, the GEO-iSHAI stability indices have a great added value because SEVIRI provides useful spatial and temporal resolution. It is important to take into account that a certain degree of disagreement between ECMWF analysis and real temperature and humidity profiles always exists. For this reason, this is not always a negative aspect that the statistical values in BT_SEVIRI case are greater than the ones in BT_RTTOV case because it reflects the fact that real SEVIRI BTs from the real world are not the same that the synthetic and ideal RTTOV BTs (*t+00*). One of the added values of the GEO-iSHAI is to show where and when there is a disagreement between ECMWF forecast or analysis against the real bias corrected SEVIRI BTs retrieved profiles. Thus, the GEO-iSHAI stability parameters are able to delimitate the region

where instability is growing before convection is triggered, as it can be seen on the study case loops or in the near real time loops in http://nwc-saf.eumetsat.int.

LI sea	NWPHyb(t+24)	FG	Phy. Retrieval
RMSE (ºC)	0,918	0,900	0,900
BIAS (ºC)	-0,079	-0,066	-0,065
SHW sea	NWPHyb(t+24)	FG	Phy. Retrieval
RMSE (ºC)	1,580	1,517	1,507
BIAS (ºC)	-0,180	-0,043	-0,037
KI sea	NWPHyb(t+24)	FG	Phy. Retrieval
RMSE (ºC)	4,699	4,496	4,400
BIAS (ºC)	0,360	0,168	0,150

LI land	NWPHyb(t+24)	FG	Phy. Retrieval
RMSE (ºC)	0,938	0,923	0,917
BIAS (ºC)	0,081	0,118	0,121
SHW land	NWPHyb(t+24)	FG	Phy. Retrieval
RMSE (ºC)	1,035	1,020	1,009
BIAS (ºC)	0,050	0,108	0,118
KI land	NWPHyb(t+24)	FG	Phy. Retrieval
RMSE (ºC)	3,716	3,577	3,455
BIAS (ºC)	-0,226	-0,386	-0,455

*Table 5: **BT_RTTOV case:** Statistical parameters for Lifted Index (LI), Showalter Index (SHW) and K Index (KI) parameters over the Full Disk validation points in year 2017 dataset. Left) sea pixels, right) land pixels.*

LI sea	NWPHyb(t+24)	FG	Phy. Retrieval
RMSE (ºC)	0,918	0,907	0,907
BIAS (ºC)	-0,079	-0,028	-0,023
SHW sea	NWPHyb(t+24)	FG	Phy. Retrieval
RMSE (ºC)	1,198	1,150	1,134
BIAS (ºC)	-0,180	-0,038	-0,023
KI sea	NWPHyb(t+24)	FG	Phy. Retrieval
RMSE (ºC)	3,439	3,323	3,227
BIAS (ºC)	0,360	0,155	0,098

LI land	NWPHyb(t+24)	FG	Phy. Retrieval
RMSE (ºC)	0,938	0,933	0,936
BIAS (ºC)	0,081	0,048	0,056
SHW land	NWPHyb(t+24)	FG	Phy. Retrieval
RMSE (ºC)	0,655	0,673	0,726
BIAS (ºC)	0,050	0,050	0,064
KI land	NWPHyb(t+24)	FG	Phy. Retrieval
RMSE (ºC)	2,283	2,285	2,384
BIAS (ºC)	-0,226	-0,222	-0,307

*Table 6: **BT_SEVIRI case:** Statistical parameters for Lifted Index (LI), Showalter Index (SHW) and K Index (KI) parameters over the Full Disk validation points in year 2017. Left) sea pixels, right) land pixels.*

3.6 VALIDATION OF GEO-iSHAI TOZ: TOTAL OZONE

In this Section the validation results of the Total Ozone (TOZ) are shown.

GEO-iSHAI TOZ output was introduced as a new output in release 2016 and TOZ was calculated from the ozone profile after applying only the non-linear regression step. In version 2016 in the ozone non-linear regressions, the collocated real bias corrected BTs and the temperature profile, the logarithm of ozone profile and the skin temperature from background NWP profile were used as inputs.

Thus, neither the physical retrieval step nor the iSHAI retrieved profile (result of FG or physical retrieval step depending on BT_RMS_THREHOLD keyword) were not used in the ozone profile estimation.

In version 2018; this has been changed and in the ozone non-linear regressions, the collocated real bias corrected and the temperature profile, the logarithm of specific humidity profile and the skin temperature from the iSHAI retrieved profile and the logarithm of ozone profile from the background NWP profile are used as inputs. See the ATBD [RD.3] for more details. Also in version 2018 it has been recalculated the regression coefficients with 2017 year GEO–iSHAI validation and training dataset.

In Figure 17 the ozone profile rmse between background NWP-Hyb *t+24* forecast and the analysis *t+00* (***black line***) and the ozone profile rmse between the estimated GEO-iSHAI ozone and the analysis are shown. In order to compare the performances using the non-linear regression for ozone profile from the background NWP profile and from the iSHAI retrieved profile it has been shown in the figures the performances labelling as FG case (**green lines**) the use as NWP input of the background NWP profile and PHY case (**red lines**) the use as NWP input of the end iSHAI retrieved profile.

As can be seen from the figures 17 to 20 the use of the end iSHAI temperature profile, specific humidity profile and SKT instead of the ones from the background NWP does not deteriorate the TOZ performances.

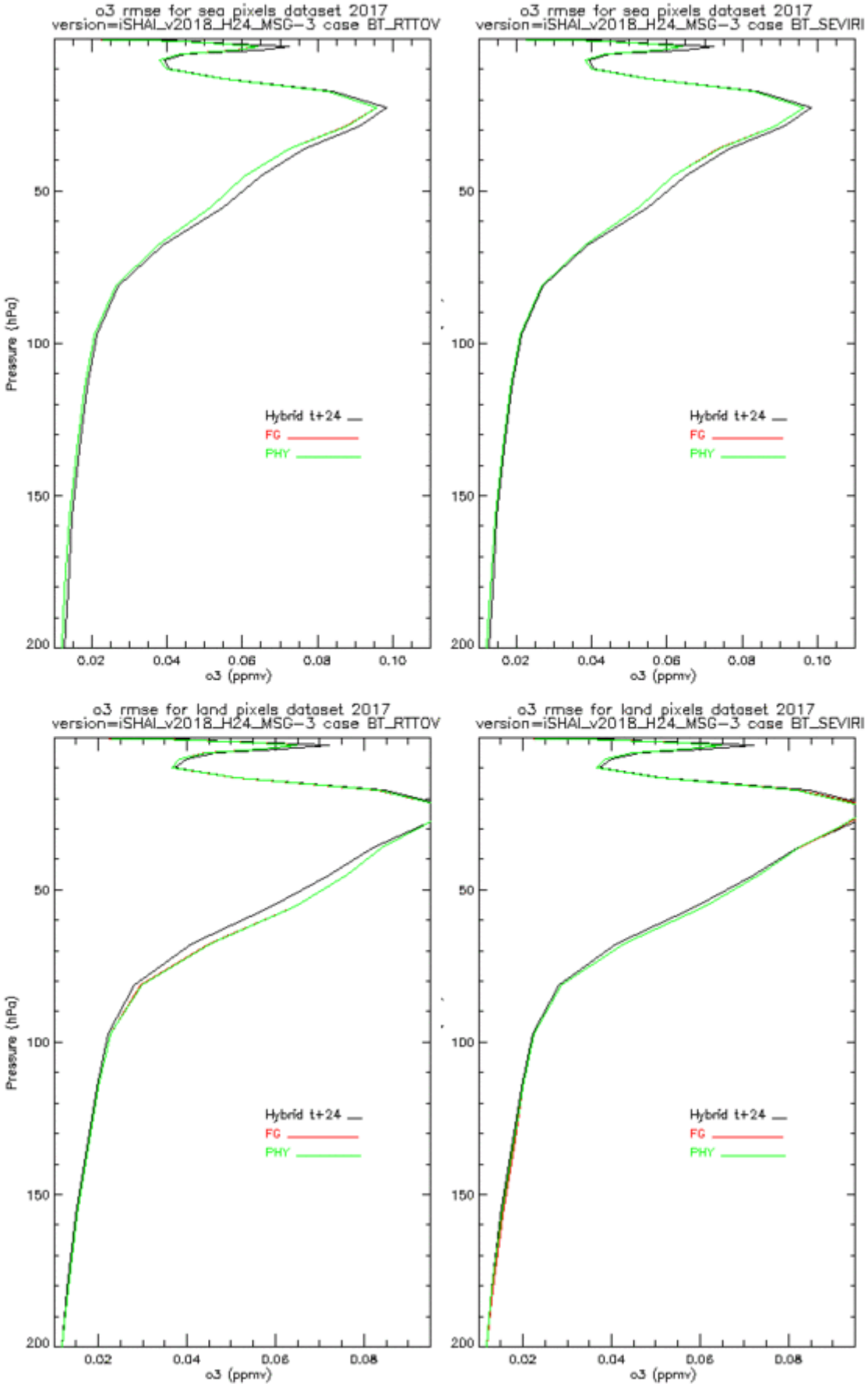

Figure 17: RMSE of ozone profiles (ppmv) at different steps compared with ECMWF analysis (t+00) hybrid profiles. Left) BT_RTTOV case, right) BT_SEVIRI case. Top) RMSE of ozone over sea pixels, bottom) RMSE of ozone over land pixels.

In Figure 18 the spatial ozone rmse between background NWP-Hyb *t+24* forecast and the analysis and the ozone profile rmse between the estimated GEO-iSHAI ozone and the analysis are shown. There is not any region with degraded performance and BT_SEVIRI and BT_RTTOV spatial performance are similar.

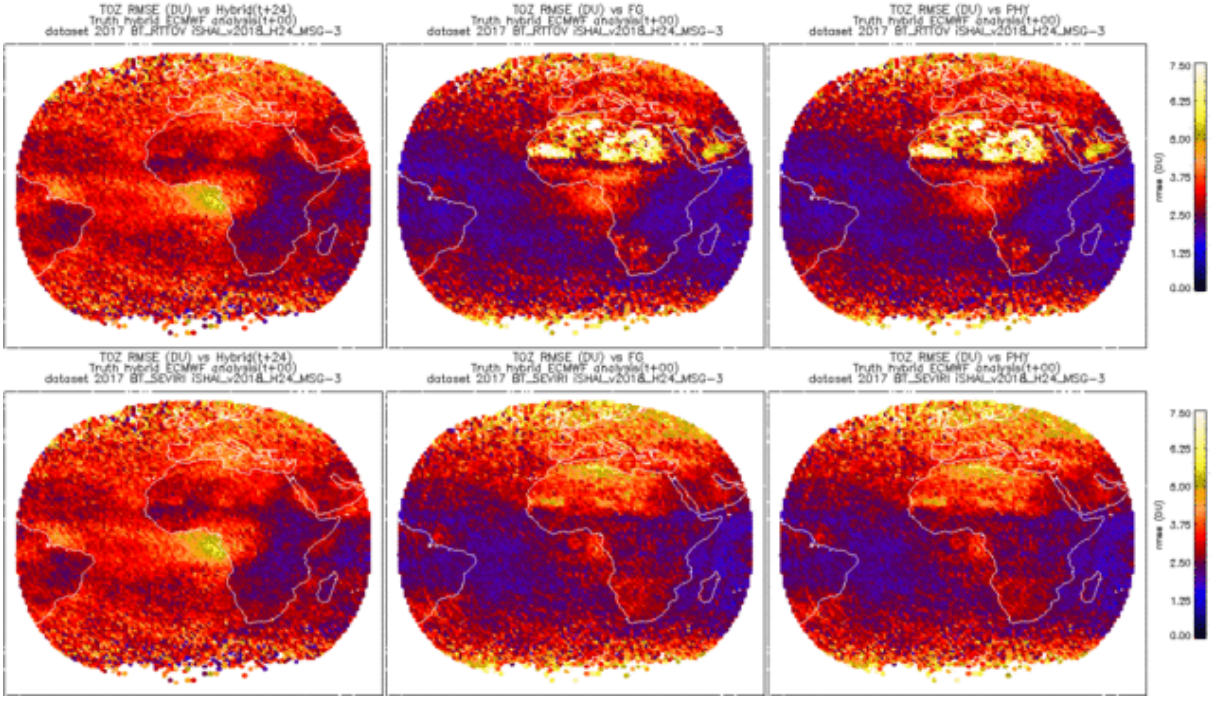

Figure 18: Spatial distribution of the TOZ RMSE over validation points in 2017 dataset. (top) BT_RTTOV case (bottom) BT_SEVIRI case. Left) TOZ RMSE calculated directly from background ECMWF hybrid GRIB (t+24), centre) GEO-TOZ RMSE calculated after non-linear regression step profile from the background profile, right) GEO-TOZ RMSE calculated after non-linear regression step profile from the end iSHAI profile. In all case the ground truth are TOZ calculated from NWP-Hyb ECMWF analysis(t+00) profiles.

In Figures 19 and 20 the two dimensional histograms for TOZ between background NWP-Hyb *t+24* forecast and the analysis and between the estimated GEO-iSHAI TOZ and the analysis TOZ are shown. It can be seen that the two dimensional histograms of TOZ from BT_SEVIRI case are similar to the ones for BT_RTTOV case and this confirms the results of Figures 17 and 18.

The statistical values (RMSE, bias and correlation) that appear in the 2D histograms are also written at the end of this Section 3.5 for a more comfortable read and comparison in Tables 7 and 8.

The reductions on TOZ rmse over sea in the BT_RTTOV case are of 20% and 15% on BT_SEVIRI case. Over land pixel it can be seen one degradation of 18 % in BT_RTTOV case are but only of 6% on BT_SEVIRI case. The different behaviour in sea and land pixels is likely due to emissivity and skin temperature errors in land pixels inputs. Other time, this represents the difference between synthetic RTTOV case and real SEVIRI case.

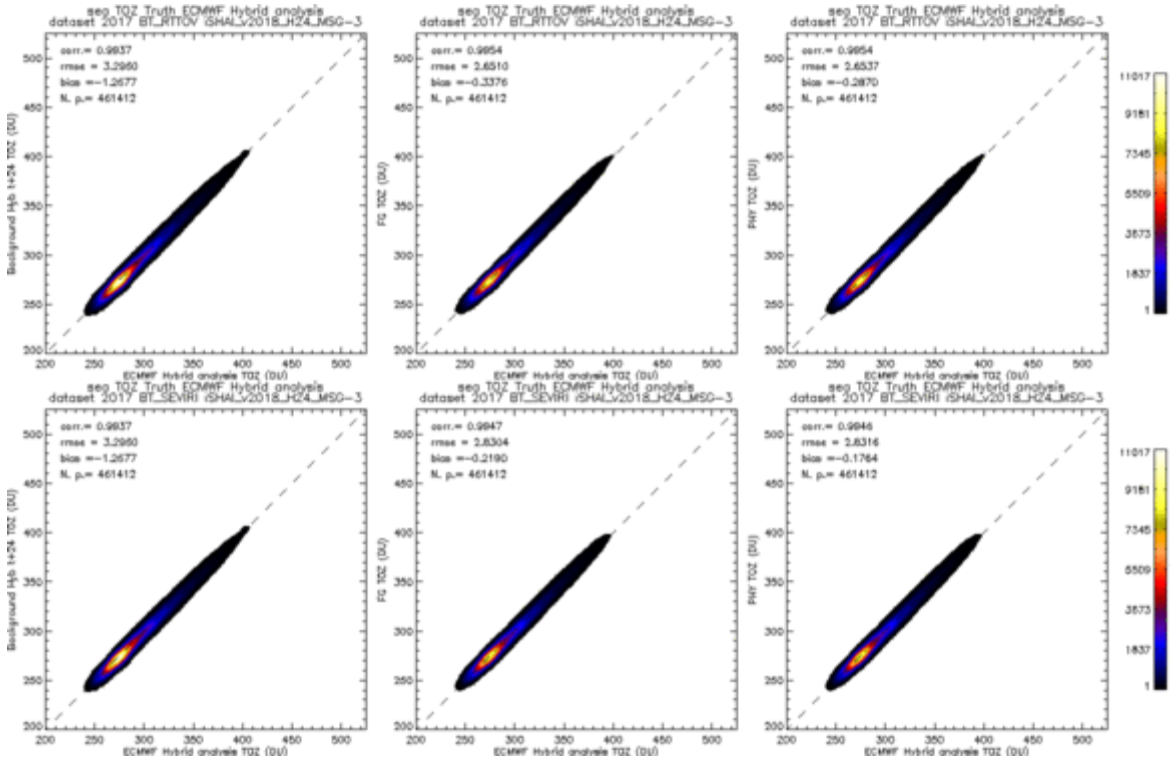

*Figure 19: **Sea** case TOZ 2D histograms. (top) BT_RTTOV case. (bottom) BT_SEVIRI case. Left) TOZ calculated directly from background t+24 ECMWF hybrid GRIB centre) TOZ calculated after non-linear regression step profile from the background profile, right) TOZ RMSE calculated after non-linear regression step profile from the end iSHAI profile.*

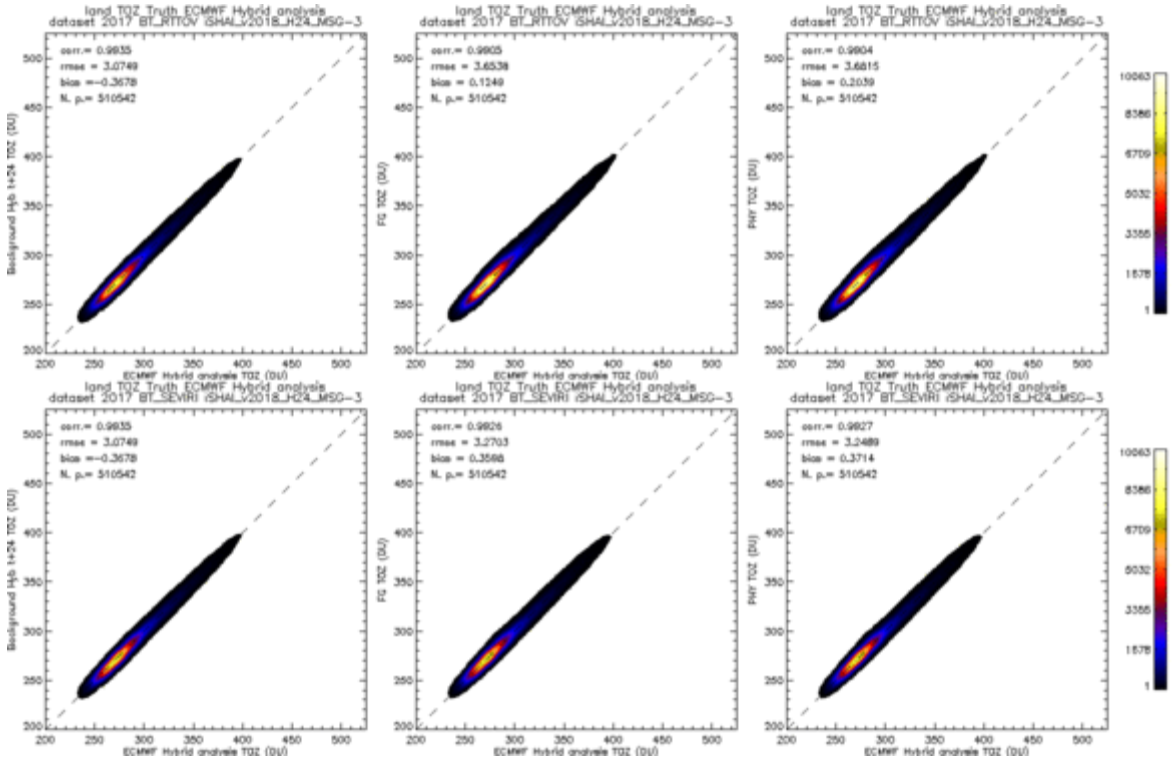

*Figure 20: **Land** case TOZ 2D histograms. (top) BT_RTTOV case. (bottom) BT_SEVIRI case. Left) TOZ calculated directly from background t+24 ECMWF hybrid GRIB centre) TOZ calculated after non-linear regression step profile from the background profile, right) TOZ RMSE calculated after non-linear regression step profile from the end iSHAI profile.*

TOZ sea	NWPHyb(*t+24*)	FG O_3_regression(t+24)	PHY O_3_regression(iSHAI)
RMSE (DU)	3,296	2,651	2,654
BIAS (DU)	-0,338	-0,287	-0,368

TOZ land	NWPHyb(*t+24*)	FG O_3_regression(t+24)	PHY O_3_regression(iSHAI)
RMSE (DU)	3,075	3,654	3,681
BIAS (DU)	0,125	0,204	0,000

*Table 7: **BT_RTTOV case:** Statistical parameters for Total Ozone (TOZ) parameter over the Full Disk validation points in year 2017. Left) sea pixels, right) land pixels.*

TOZ sea	NWPHyb(*t+24*)	FG O_3_regression(t+24)	PHY O_3_regression(iSHAI)
RMSE (DU)	3,296	2,830	2,832
BIAS (DU)	-0,219	-0,176	-0,368

TOZ land	NWPHyb(*t+24*)	FG O_3_regression(t+24)	PHY O_3_regression(iSHAI)
RMSE (DU)	3,075	3,270	3,249
BIAS (DU)	0,360	0,371	0,000

*Table 8: **BT_SEVIRI case:** Statistical parameters for Total Ozone (TOZ) parameter over the Full Disk validation points in year 2017. Left) sea pixels, right) land pixels.*

3.7 VALIDATION OF GEO-iSHAI SKT: SKIN TEMPERATURE

In this Section the validation results of the Skin Temperature (SKT) are shown. This GEO-iSHAI output was introduced as a new output in release 2016. Below, the Tables and Figures with the statistical parameters for the SKT parameters are shown. SKT is written just for nowcasting purposes and in order for the users to have access to this parameter. As an example, as SKT is used in the RTTOV calculations, the inspection of spatial gradients and temporal tendency could be used to detect the presence of non-adequately detected clouds or errors in the background NWP SKT.

The SKT should be taken as an indicative output and it should not be considered as SST or LST products because more controls and spatial and temporal tests would be needed. The SKT field of ECMWF has not a great quality especially over land pixels; due to this fact the spatial rmse in BT_SEVIRI case show great values over land in Figure 23. The result of the Figures and Tables in this SKT Section is that GEO-iSHAI SKT could be used to inform users of the discrepancies between the background NWP SKT and one optimal SKT in the pixels; but it must be taken into account that the discrepancies could be due to physical reasons, due to undetected clouds or due to error in the emissivities, etc.

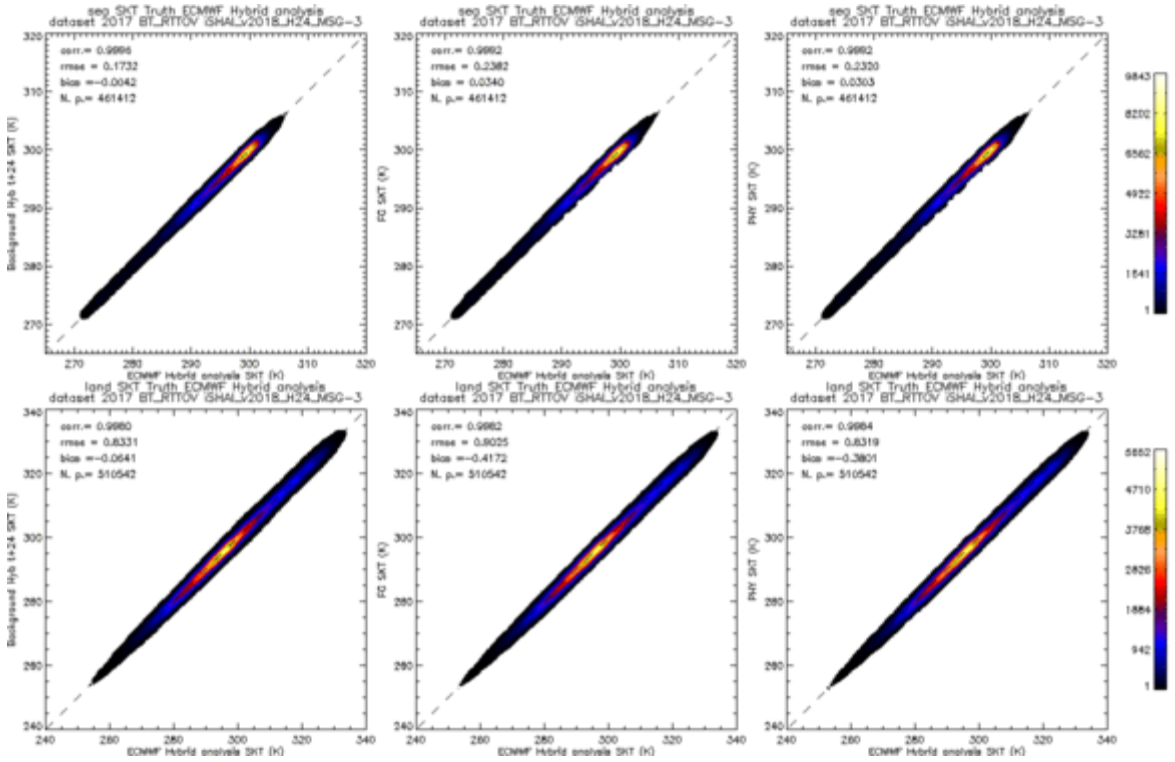

*Figure 21: **BT_RTTOV** case SKT 2D histograms. (top) sea SKT. (bottom) land SKT. Left) SKT RMSE calculated directly from background ECMWF hybrid GRIB (t+24), centre) SKT RMSE calculated after FG step profile, right) SKT RMSE calculated after physical retrieval step profile. In all case the ground truth is SKT calculated from NWP-Hyb ECMWF analysis(t+00) profiles.*

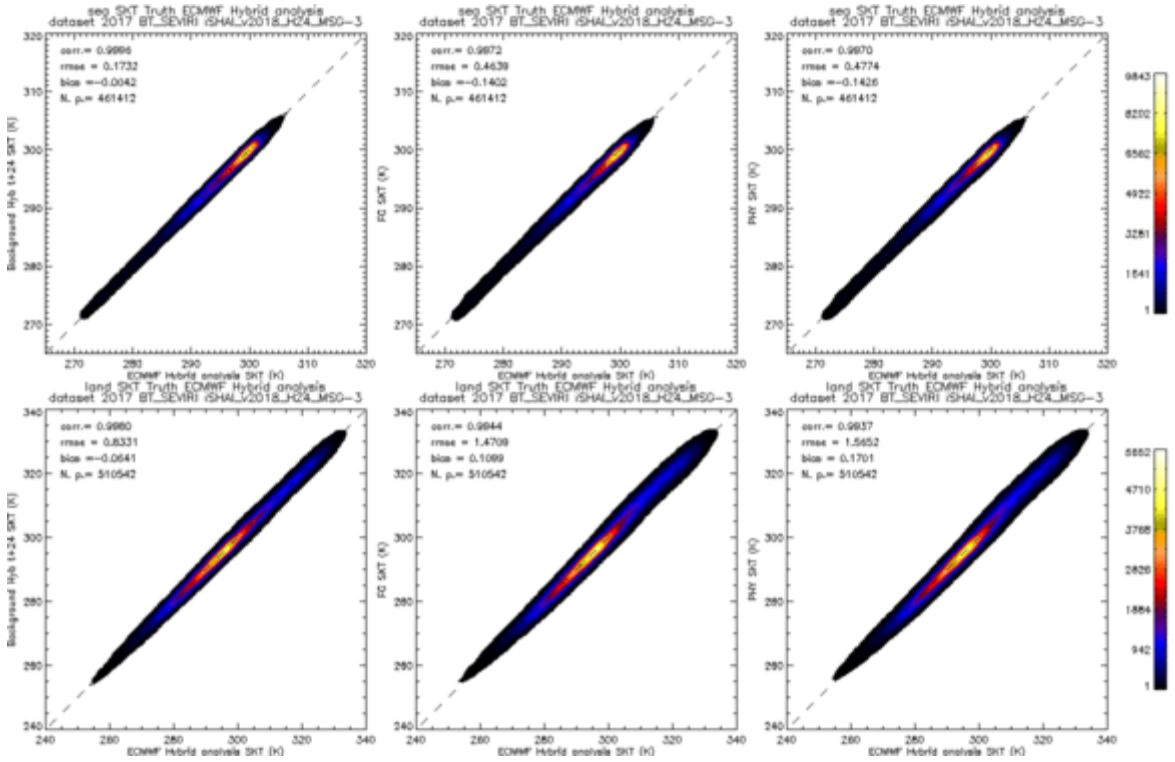

*Figure 22: **BT_SEVIRI** case SKT 2D histograms. (top) sea SKT. (bottom) land SKT. Left) SKT RMSE calculated directly from background ECMWF hybrid GRIB (t+24), centre) SKT RMSE calculated after FG step profile, right) SKT RMSE calculated after physical retrieval step profile. In all case the ground truth is SKT calculated from NWP-Hyb ECMWF analysis(t+00) profiles.*

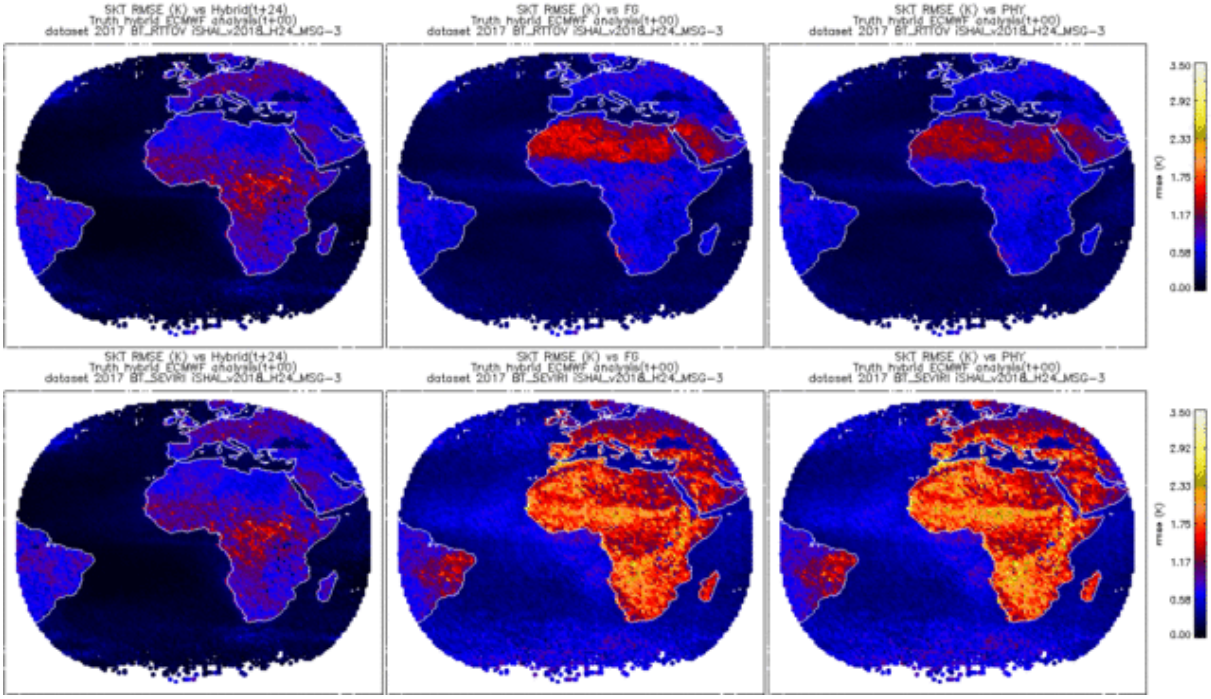

Figure 23: Spatial distribution of the SKT RMSE. (top) BT_RTTOV case (bottom) BT_SEVIRI case. Left) TOZ RMSE calculated directly from background ECMWF hybrid GRIB (t+24), (centre) SKT RMSE calculated after FG non-linear regression step,(right) GEO-SKT RMSE calculated after physical retrieval step. In all case the ground truth are SKT calculated from NWP-Hyb ECMWF analysis(t+00) profiles.

SKT sea	NWPHyb(*t+24*)	FG	Phy. Retrieval
RMSE (K)	0,173	0,238	0,232
BIAS (K)	-0,004	0,034	0,030

SKT land	NWPHyb(*t+24*)	FG	Phy. Retrieval
RMSE (K)	0,833	0,903	0,832
BIAS (K)	-0,064	-0,417	-0,380

*Table 9: **BT_RTTOV case:** Statistical parameters for Skin Temperature (SKT) parameter over the Full Disk validation points in year 2017. Left) sea pixels, right) land pixels.*

SKT sea	NWPHyb(*t+24*)	FG	Phy. Retrieval
RMSE (K)	0,173	0,464	0,477
BIAS (K)	-0,004	-0,140	-0,143

SKT land	NWPHyb(*t+24*)	FG	Phy. Retrieval
RMSE (K)	0,833	1,471	1,565
BIAS (K)	-0,064	0,110	0,170

*Table 10: **BT_SEVIRI case:** Statistical parameters for Skin Temperature (SKT) parameter over the Full Disk validation points in year 2017. Left) sea pixels, right) land pixels.*

4. VALIDATION RESULTS ON AHI BT_RTTOV TEST

In this section the early results of the first GEO-iSHAI validation of AHI instrument on board Himawari using synthetic RTTOV simulation from SEVIRI GEO-iSHAI validation and training dataset profiles but simulated using the AHI channels with RTTOV is shown. In CDOP-3 more Scientific Reports with AHI using real AHI BTs will be written.

The histograms with `BT_distance` and with `BT_RMS` for the AHI BT_RTTOV test at the different steps of the GEO iSHAI module are shown in Figure 24. It can be seen that the physical retrieval step reduces significantly the number of profiles with `BT_distance` and `BT_RMS` greater than 0.6 and the performance is slightly better than the histograms in SEVIRI BT_RTTOV case.

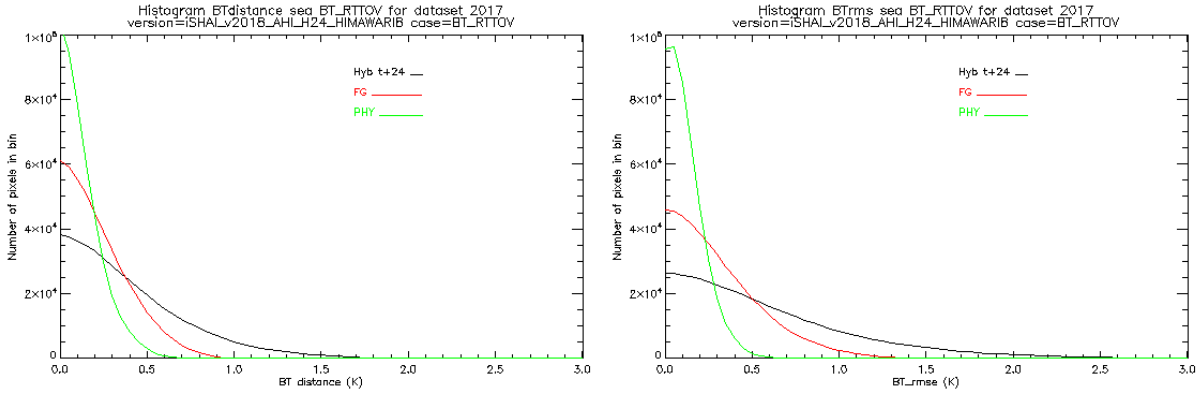

Figure 24: AHI BT_RTTOV test: Histogram of left) `BT_distance` *(distance in all AHI channels channels) and right)* `BT_RMS` *(distance in absorption channels) at different steps of GEO-iSHAI on synthetic AHI BT_RTTOV case on sea pixels.*

The comparison of RMSE q profiles in Figure 25 of AHI BT_RTTOV test with the ones in Figure 7 and 8 on SEVIRI BT_RTTOV test shows on slight improvement in AHI BT_RTTOV test; the availability of the third WV channel does not significantly increases the performance in AHI BT_RTTOV test.

The comparison of LPW and TPW 2D histograms in Figures 26 and 27 of AHI BT_RTTOV test with the ones in Figures 9 and 10 on SEVIRI BT_RTTOV test shows on slight improvement in AHI BT_RTTOV test. Same conclusion can be drawn; the availability of the third WV channel does not significantly increases the performance of GEO-ISHAI in AHI BT_RTTOV test.

The comparison of spatial RMS of LPW and TPW in Figures 28 and 29 of AHI BT_RTTOV test with the ones in Figures 13 and 14 on SEVIRI BT_RTTOV test shows the same spatial pattern with very slight improvement in AHI BT_RTTOV test.

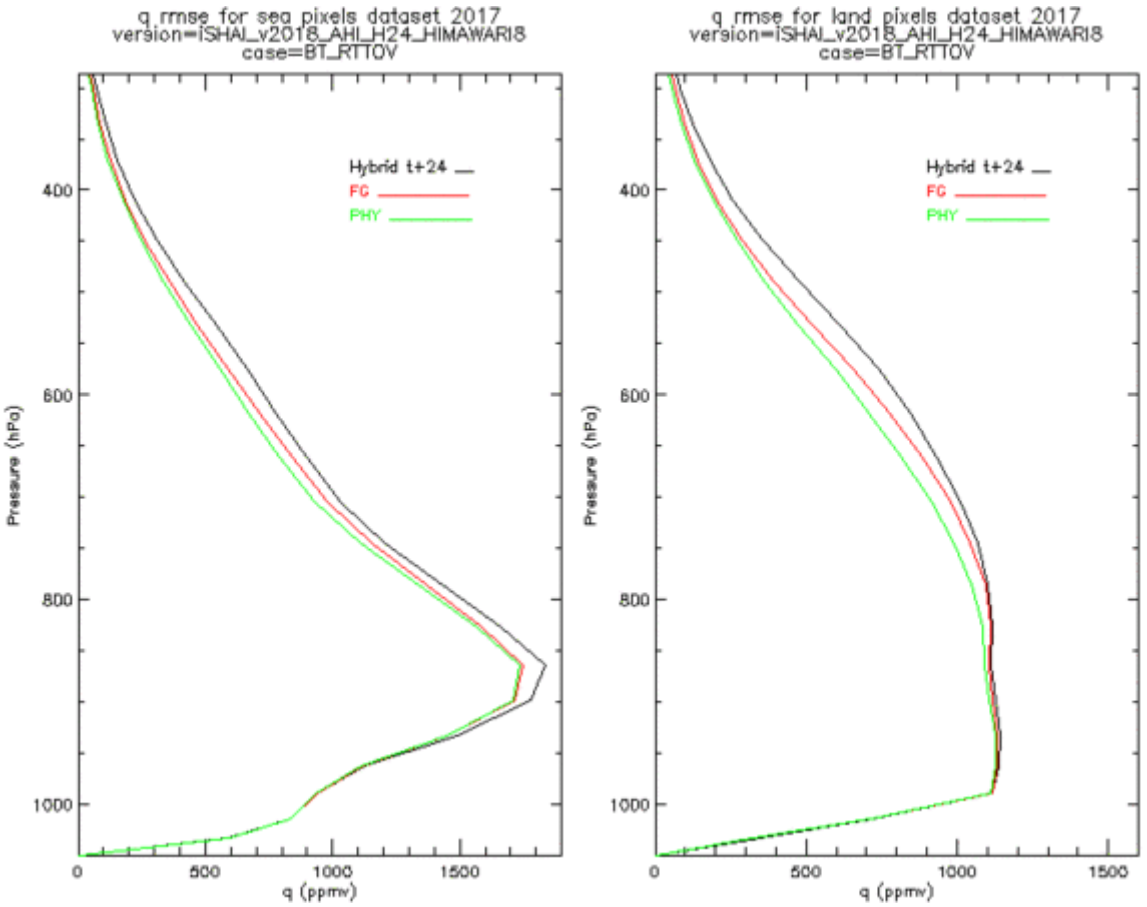

Figure 25: AHI BT_RTTOV test: RMSE q profiles (ppmv) at different steps compared with ECMWF analysis (t+00) hybrid profiles. Left) over sea pixels, right) over land pixels

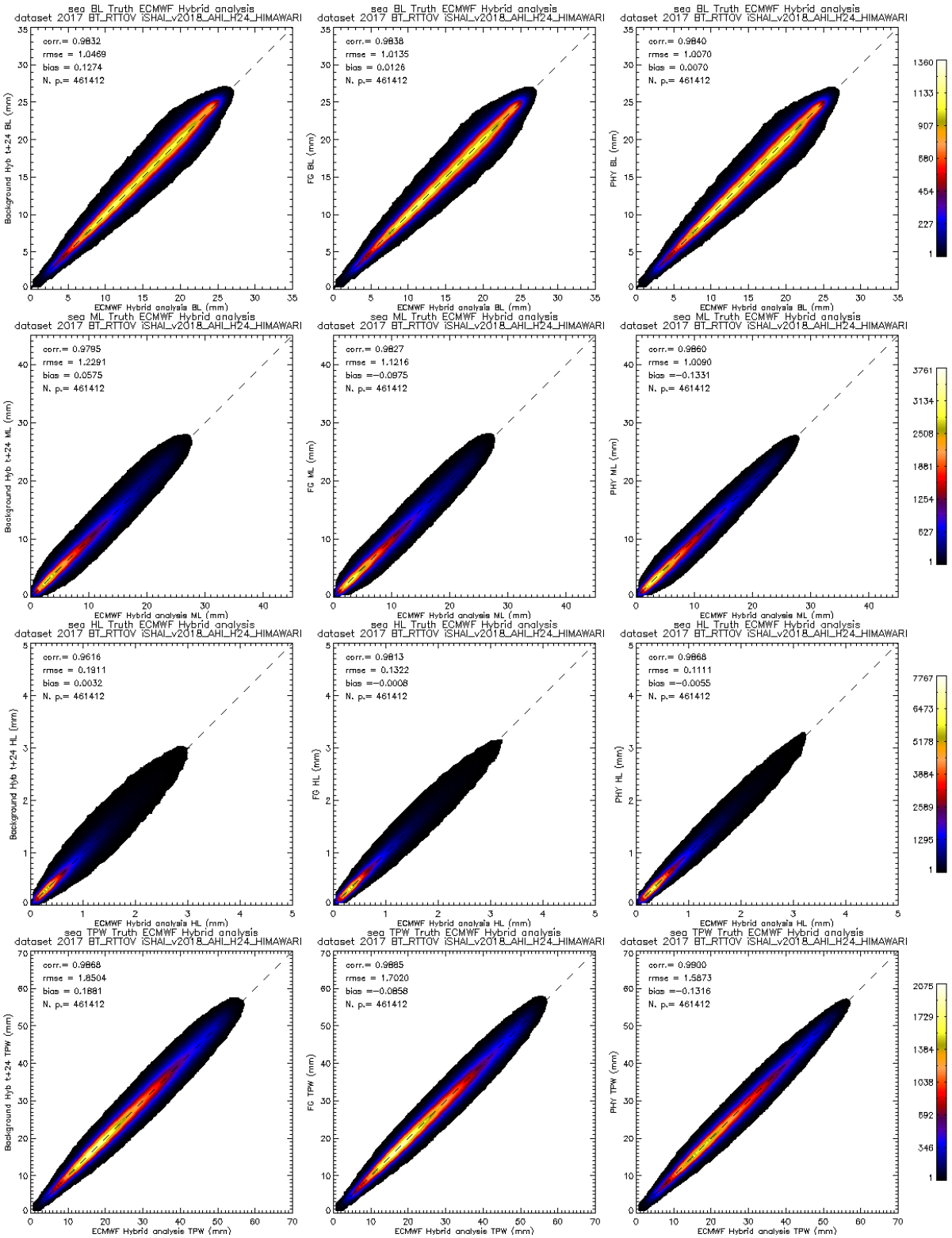

*Figure 26: **AHI BT_RTTOV test**: LPW and TPW 2D histograms over **sea** validation points. From top to bottom BL, ML, HL and TPW parameters. Left) BL, ML, HL and TPW parameters calculated directly from background ECMWF from hybrid profiles from (t+24) forecast, centre) BL, ML, HL and TPW parameters calculated after FG step profile using as input AHI BT_RTTOV (t+00), right) BL, ML, HL and TPW parameters calculated after physical retrieval step profile over sea AHI RTTOV BTs. In all case the ground truth are the BL, ML, HL and TPW calculated from ECMWF analysis (t+00) profiles.*

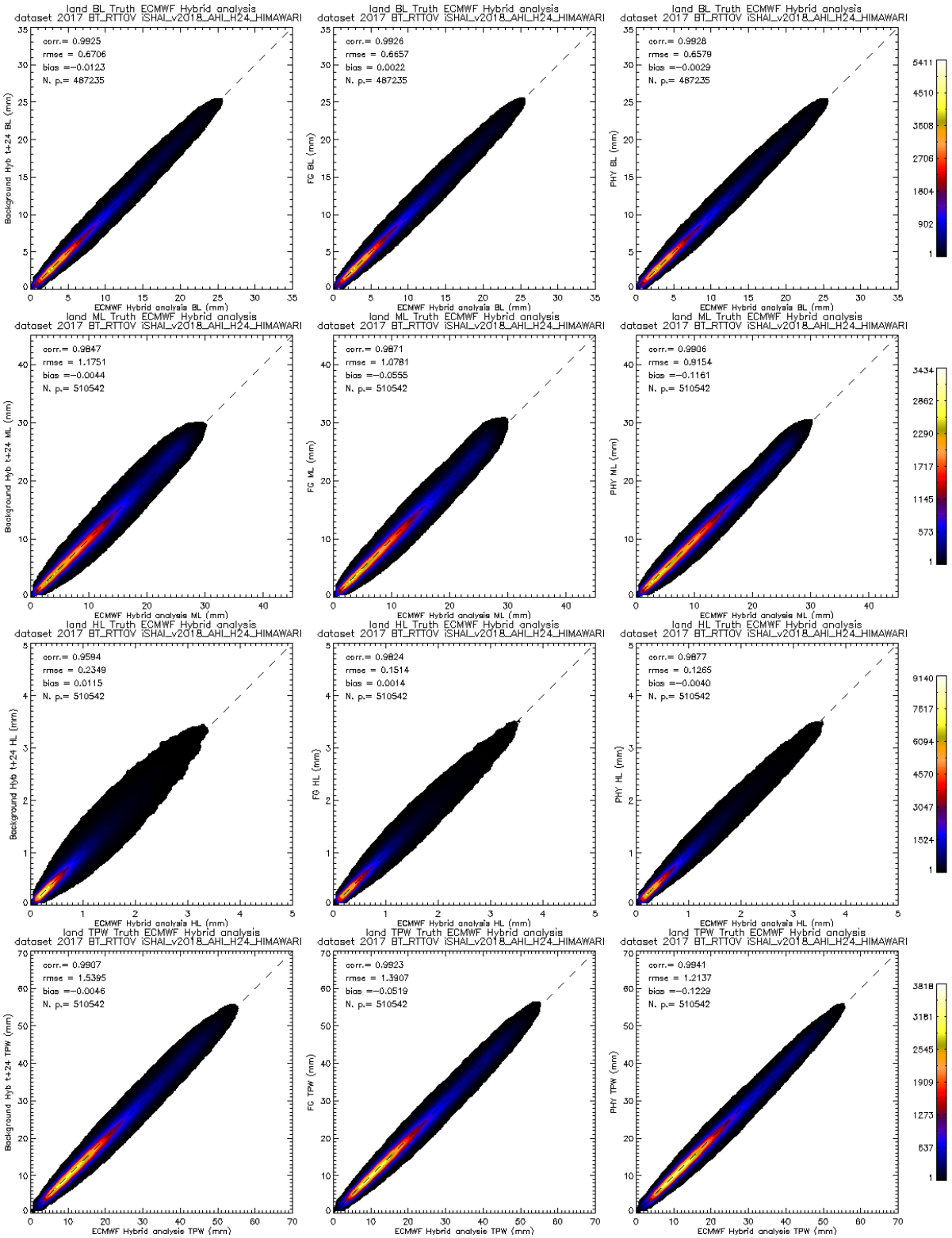

*Figure 27: **AHI BT_RTTOV test**: LPW and TPW 2D histograms over **land** validation points. From top to bottom BL, ML, HL and TPW parameters. Left) BL, ML, HL and TPW parameters calculated directly from background ECMWF from hybrid profiles from (t+24) forecast, centre) BL, ML, HL and TPW parameters calculated after FG step profile using as input AHI BT_RTTOV (t+00), right) BL, ML, HL and TPW parameters calculated after physical retrieval step profile over sea AHI RTTOV BTs. In all case the ground truth are the BL, ML, HL and TPW calculated from ECMWF analysis (t+00) profiles.*

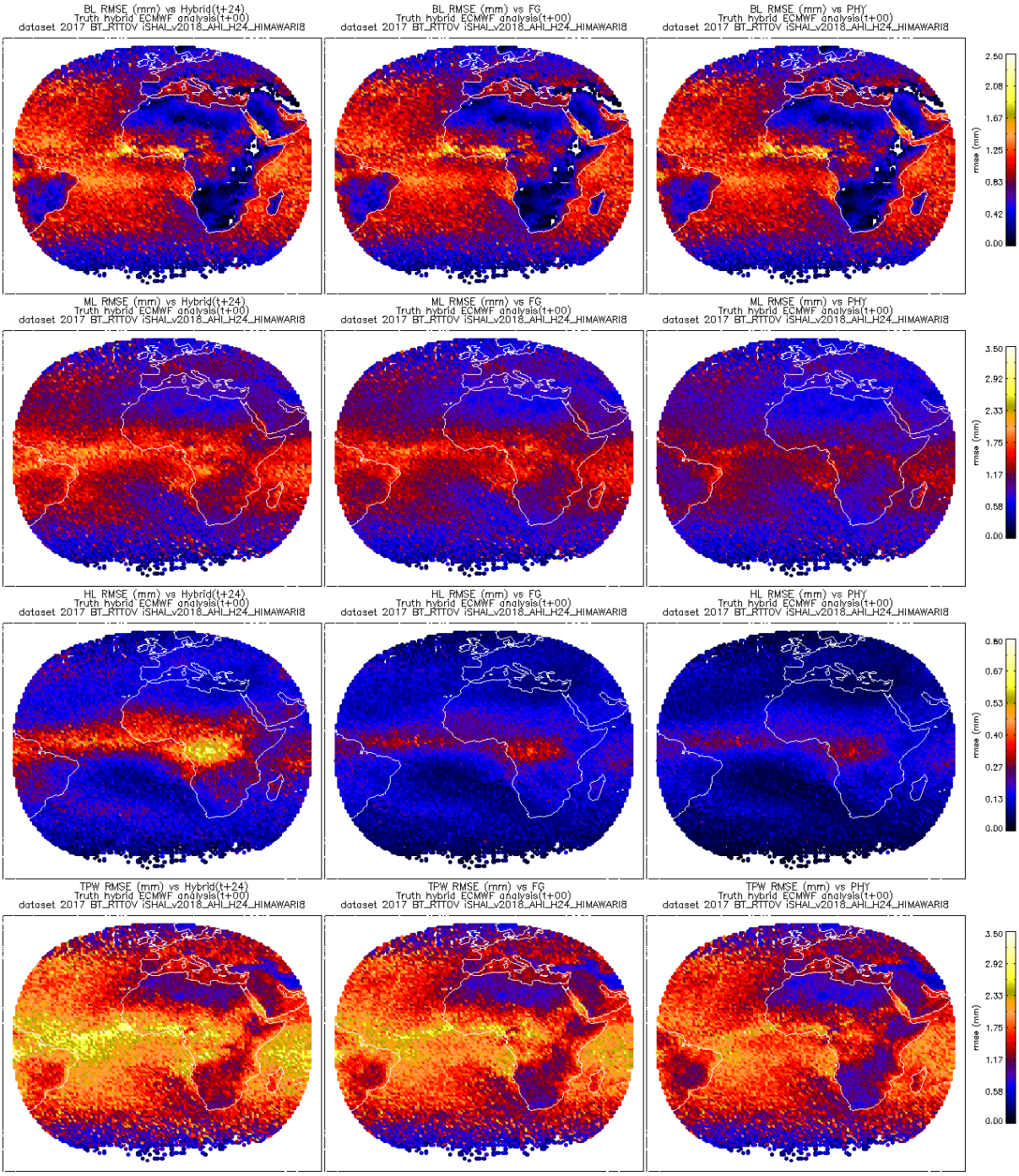

*Figure 28: **AHI BT_RTTOV test**: Spatial distribution of the BL, ML, HL and TPW RMSE over validation points in 2017 dataset. From top to bottom BL, ML, HL and TPW parameters. Left) BL, ML, HL and TPW RMSE calculated directly from background ECMWF hybrid GRIB (t+24), centre) BL, ML, HL and TPW RMSE calculated after FG step profile, right) BL, ML, HL and TPW RMSE calculated after physical retrieval step profile. In all case the ground truth are the BL, ML, HL and TPW calculated from NWP-Hyb ECMWF analysis (t+00) profiles*

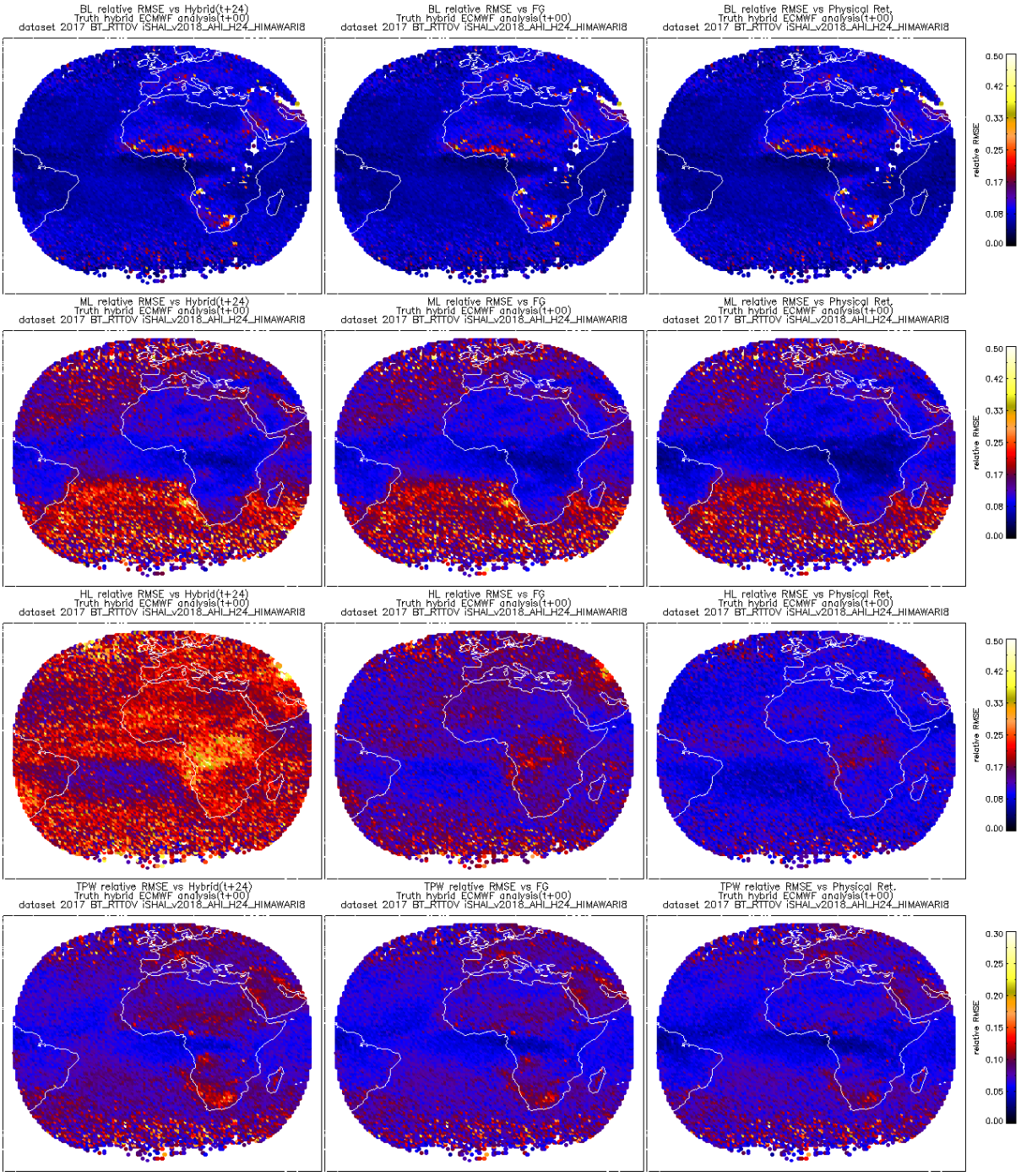

*Figure 29: **AHI BT_RTTOV test:** Same that Figure 28 but relative RMSE instead of RMSE*

The comparison of 2D histogram for SKT and spatial RMSE of SKT in Figures 30 and 31 of AHI BT_RTTOV test with the ones in Figures 20 to 22 on SEVIRI BT_RTTOV test shows one slight improvement in AHI BT_RTTOV test over sea pixels and a moderate improvement over land pixels. The moderate improvement in SKT performance is likely due to AHI has three split window channels while SEVIRI has only two split window channels.

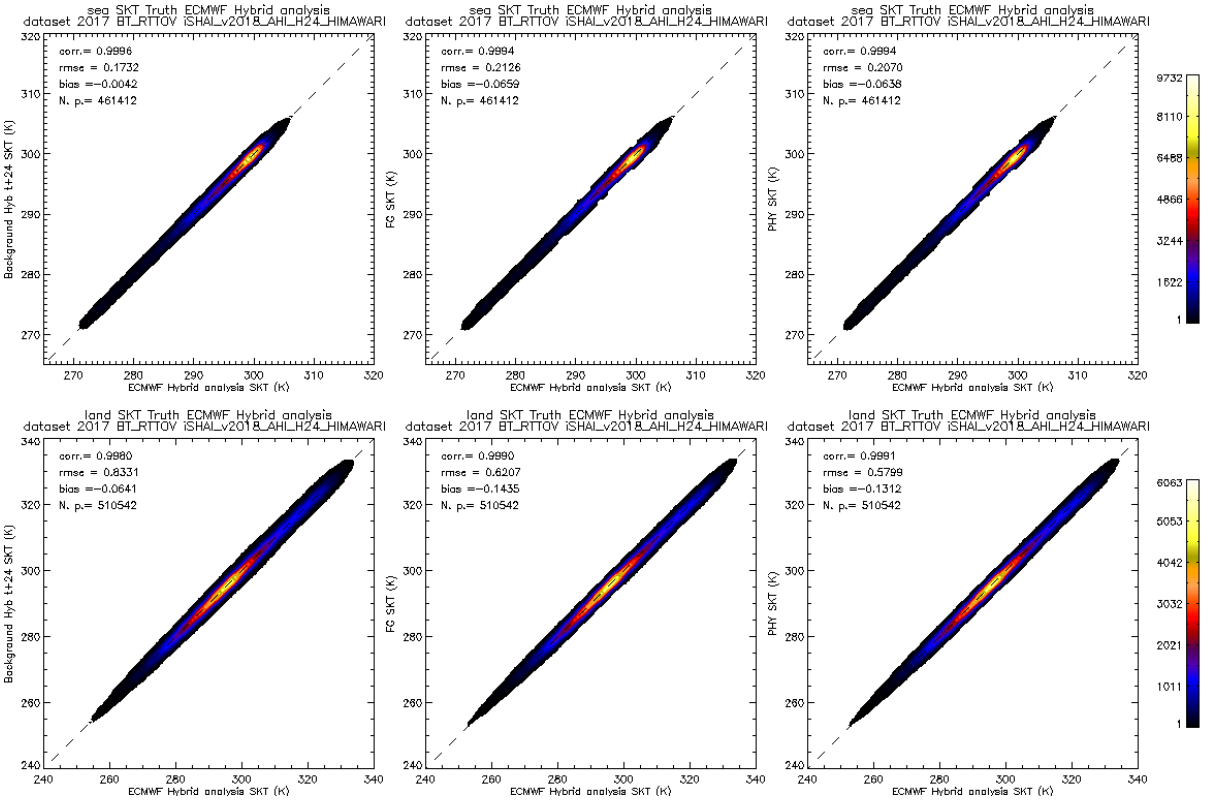

*Figure 30: **AHI BT_RTTOV test**: SKT 2D histograms. (top) sea SKT. (bottom) land SKT. Left) SKT RMSE calculated directly from background ECMWF hybrid GRIB (t+24), centre) SKT RMSE calculated after FG step profile, right) SKT RMSE calculated after physical retrieval step profile. In all case the ground truth is SKT calculated from NWP-Hyb ECMWF analysis(t+00) profiles.*

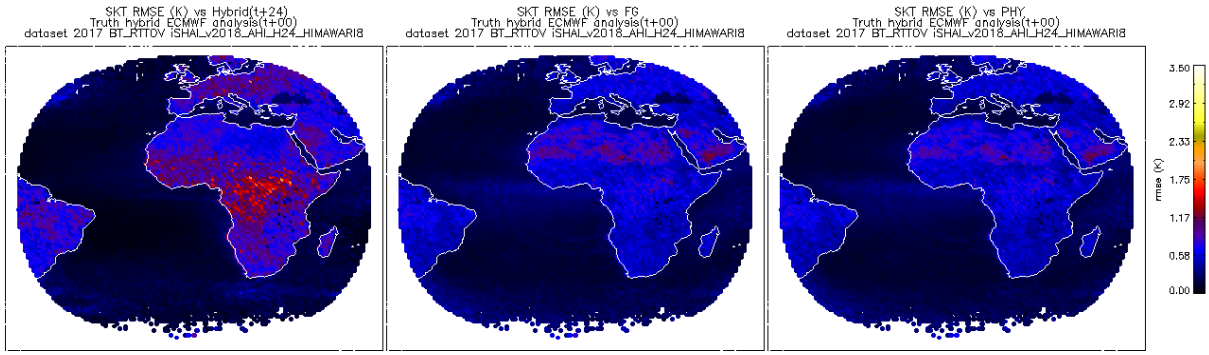

Figure 31: Spatial distribution of the SKT RMSE. (top) BT_RTTOV case (bottom) BT_SEVIRI case. Left) TOZ RMSE calculated directly from background ECMWF hybrid GRIB (t+12), (centre) SKT RMSE calculated after FG non-linear regression step,(right) GEO-SKT RMSE calculated after physical retrieval step. In all case the ground truth are SKT calculated from NWP-Hyb ECMWF analysis (t+00) profiles.

5. CONCLUSIONS

After this validation of GEO-iSHAI, some conclusions can be obtained:

- To build a good training and validation dataset is a very important and standing task for us. This continuous task has allowed the generation of a huge dataset. The use of this dataset has two main aims. The first one is to serve for the validation and tuning of the current version of the algorithm. The second one is the training, testing and validation of new versions of GEO-iSHAI. In the 2018 version all the coefficients have been calculated from the GEO-iSHAI validation and training datasets (using ECMWF profiles).
- It is needed to improve the process for screening of cloud contaminated pixels. As can be seen in Figure 34 there are still cloudy contaminated pixels that increase the rmse values on the case of real SEVIRI tests.
- The GEO-iSHAI processor with coefficients trained using the ECMWF NWP Hybrid dataset, allowing the use of ECMWF GRIB files on hybrid levels, improves strongly the performance over the regular version of the GEO-iSHAI, which uses ECMWF NWP fixed pressure fields. For the users that use ECMWF to feed NWC SAF software in real time, it is strongly recommend to make the effort of downloading from the MARS the ECMWF GRIB files on hybrid levels and to use the GEO-iSHAI HYB mode. For the users that use their own NWP models to feed NWC SAF software in real time, it is strongly recommended they make the effort to provide optimal vertical resolution to GEO-iSHAI.
- The performance of the regular GEO iSHAI version 2018 with fixed pressure NWP input will tend to be similar than the one for the GEO-iSHAI hybrid mode if the number of available fixed pressure vertical levels increases. Then, it is strongly recommend to the users to feed to the regular GEO iSHAI inputs with the highest available number of fixed pressure levels.
- It is also recommended to feed the GEO-iSHAI with the highest possible temporal and spatial resolution.
- Validation has been performed for the complete SEVIRI disc.
- Best results are obtained for humidity in medium layers due to the contribution of the water vapor channels. In this layer the GEO-iSHAI improves the information beyond the background NWP on the humidity profile.
- GEO imager satellites has limited information to improve the vertical information beyond the forecast, but it does provide useful spatial and temporal information. This limitation is clear for the vertical information of temperature and stability indices.
- The RMSE of the GEO iSHAI parameters are excellent (see Table 11 and Table 12 below) and all the parameters are better than is requested in the Product Requirement Document [AD.4]
- A good BT bias correction is essential for GEO-iSHAI. A mechanism to calculate and distribute frequently and updated SEVIRI BT bias correction has been implemented through a web page in the NWC SAF web, to provide frequent and rapid updates of the SEVIRI BT bias correction. A similar mechanism is being developed for AHI and ABI.
- Validation has been performed for an extended period of a complete year 2017. But there are more years available.
- A web page is being created in order to maintain updated and detailed validation documentation, examples, repository of case studies, etc.
- Tables 12 and 13 summarizes the objective validation results in terms of RMSE for SEVIRI; it summarizes the statistical values reported along the different sections of the document but the most important is that these figures represent a reduction in the RMSE from the background NWP, that on synthetic case could be greater than 50% for HL layer and 25 % for ML layer.

- This reduction of RMSE is lower using real bias corrected SEVIRI BTs due to noise of the satellite, errors in radiative transfer models and bias correction, lack of good emissivity atlases, etc and the lack of a real truth. But the algorithm is sensible to discrepancy between synthetic and real SEVIRI BTs and then is able to advice the users of any discrepancy in the forecast NWP used as background NWP; it is recommend the use of the parameters with the differences between the NWP used as input to GEO iSHAI and the retrieved profiles in order to detect any discrepancy between the forecast model and the real observations of the SEVIRI images.
- The initial validation of AHI in synthetic RTTOV case over SEVIRI 2017 training and validation dataset shows that the performance is slightly better due to the addition of two channels. For a wider improvement of SHAI products it will be needed to wait to MTG-IRS era.
- The generalization of the validation process from SEVIRI to AHI and ABI has allowed to improve the software and it has been identified and isolate the key part in order to change from one instrument to other. This advance will be used in next future to generalize the validation to MTG-FCI and later to MTG-IRS.

GEO iSHAI V4.0 summary of validation Results	Precipitable Water Low Layer – **BL RMSE**	Precipitable Water Medium Layer **ML RMSE**	Precipitable Water High Layer **HL RMSE**	Precipitable Water Total **TPW RMSE**	Showalter Index **SHW RMSE**
Against ECMWF Analysis – Over Sea Full Disk validation	1,015 (kg/m^2)	1,078 (kg/m^2)	0,138 (kg/m^2)	1,669 (kg/m^2)	1,519 (K)
Against ECMWF Analysis – Over Land Full Disk validation	0,667 (kg/m^2)	1,078 (kg/m^2)	0,177 (kg/m^2)	1,603 (kg/m^2)	1,038 (K)

Table 11: Summary of the GEO iSHAI statistical parameters in 2017 using as input t+24 forecast validation dataset using as input to GEO iSHAI real SEVIRI BTs bias corrected.

GEO iSHAI V4.0 summary of validation Results	Precipitable Water Low Layer – **BL RMSE**	Precipitable Water Medium Layer **ML RMSE**	Precipitable Water High Layer **HL RMSE**	Precipitable Water Total **TPW RMSE**	Showalter Index **SHW RMSE**
Against ECMWF Analysis – Over Sea Full Disk validation	0,573 (kg/m^2)	0,587 (kg/m^2)	0,076 (kg/m^2)	0,927 (kg/m^2)	0,849 (K)
Against ECMWF Analysis – Over Land Full Disk validation	0,446 (kg/m^2)	0,691 (kg/m^2)	0,085 (kg/m^2)	0,903 (kg/m^2)	0,770 (K)

Table 12: Summary of the GEO iSHAI statistical parameters in 2017 using as input t+12 forecast validation dataset using as input to GEO iSHAI real SEVIRI BTs bias corrected.

The statistical parameter of the above tables could be compared with the statistical accuracy values defined in the Product Requirement Table (PRT). The PRT values for GEO-iSHAI has been copied in the Table 13.

PRT rms for sea pixels	TPW (mm)	BL (mm)	ML (mm)	HL (mm)	Lifted Index (°C)	Showalter Index (°C)	K Index	SKT (K)	TOZ (DU)
Threshold Accuracy	3.5	2.5	2.5	0.5	3.0	3.0	6	4	20
Target Accuracy	1.9	1.0	1.7	0.2	1.5	1.5	3.5	2.5	9
Optimal Accuracy	1.2	0.7	0.8	0.1	1.0	1.1	3.25	1.5	7.5

Table 13: Statistical accuracy values defined in the Product Requirement Table.

6. ANNEX I: VALIDATION STATISTICS OVER EUROPE REGION.

Here are collected the statistical summary of LPW over land on Europe region to show that the differences in the performance on RTTOV case and SEVIRI case are due to the issues exposed in the Section 3.1.

It has been considered as Europe region the land pixels with latitude greater than 36º N on the iSHAI validation set of 13001 validation pixels.

First the 2D histograms over land for LPW and TPW on RTTOV and SEVIRI cases on Europe are shown in Figures 32 and 33. In order to allow a better comparison, the statistical values that appear inside the 2D histograms have been collected below in Table 14.

As can be seen from the comparison of 2D histograms for land Europe cases (Figures 32 and 33) with the ones for the full disc (Figures 10 and 12), the tilt and spread on high LPW values (mainly on ML parameter) is not present and the 2D histograms are linear always.

As can be seen from the comparison of Table 14 with the Tables 3 and 4, in the case of GEO-iSHAI validation on Europe region over land pixels the performance is better than in the full disc validation. It is also present one increase in the rmse between RTTOV and SEVIRI cases but with lower rmse increment between RTTOV and SEVIRI case. This is explained due to that over Europe region the desert and tropics issues are not present.

In Table 14 it has been added two columns (red columns) with the rmse and bias in tests made using real uncorrected bias SEVIRI BT as input to GEO-iSHAI. It can be seen that if real SEVIRI BTs are not bias BT corrected all the statistical figures are worse.

From Table 14 it is also possible to conclude that:

- the algorithm is able to make correct changes in the profile as can be seen in the RTTOV case statistical figures
- the algorithm is stable since the use of real uncorrected bias SEVIRI BT introduces greater error but the rmse does not increase uncontrollably
- since the only difference between the three cases are the BTs input the increase of rmse are due to errors in not well filtered real SEVIRI BTs, emissivities issues and lack of good truth.
- the remaining levels of rmse greater on SEVIRI cases than RTTOV one are likely caused by the remaining undetected cloudy pixels inside the validations dataset. An example can be seen in Figure 34, where red pixels in the neighbourhood of cloudy pixels with large and opposite error in ML parameter in the neighbourhood of cloudy pixels. The red pixels are caused by undetected clouds or cloud contamination; in real time operations these pixels are screened out by forecasters but they are one source of great errors when calculating statistical parameters.

In future the validation will be repeated with other truth sources as radiosoundings or ground GPS receivers.

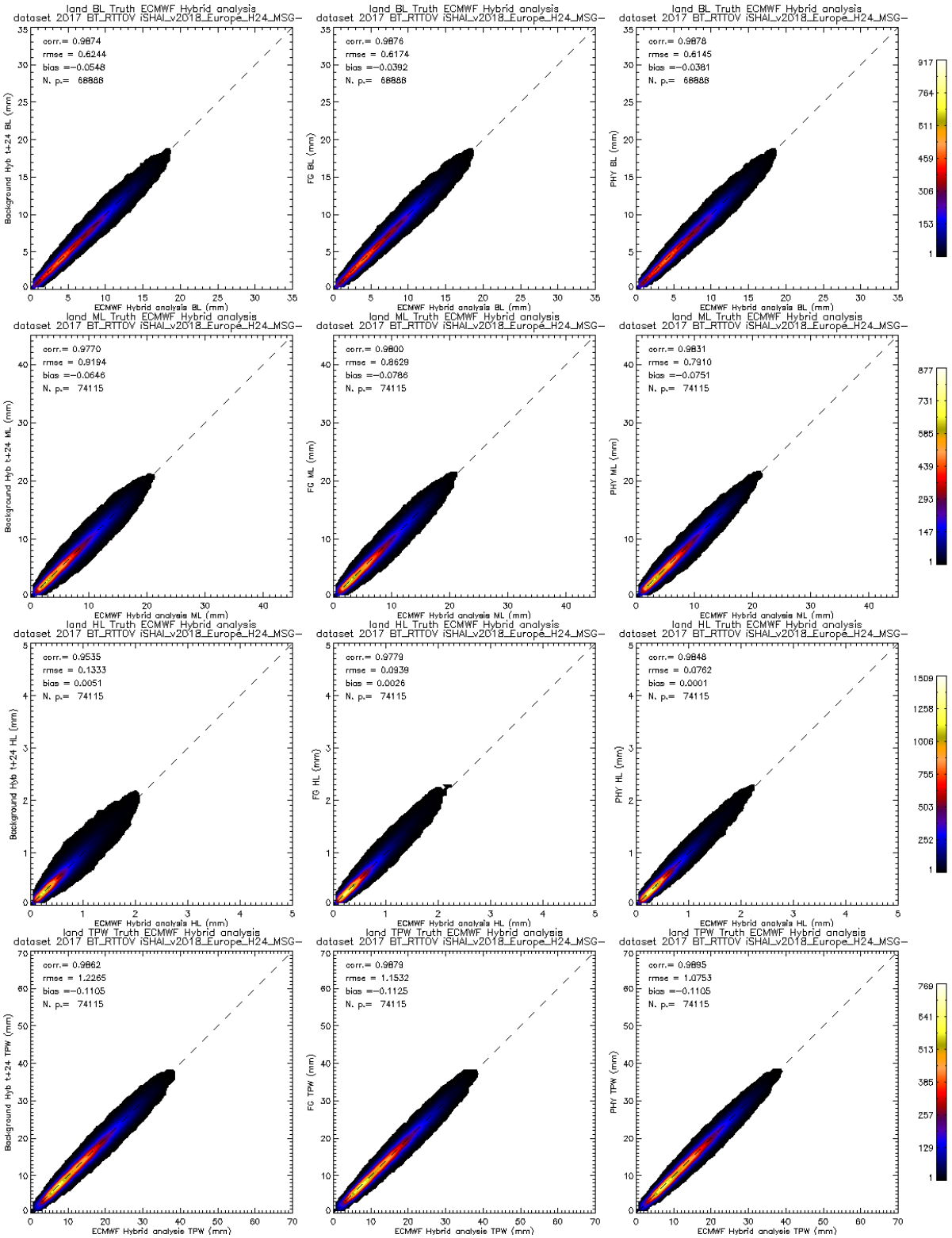

*Figure 32: **BT_RTTOV** case on Europe region: LPW and TPW 2D histograms over **land** on Europe region validation points of year 2017. From top to bottom BL, ML, HL and TPW parameters. Left) BL, ML, HL and TPW parameters calculated directly from background ECMWF from hybrid profiles from (t+24) forecast, centre) BL, ML, HL and TPW parameters calculated after FG step profile using as input using real bias corrected SEVIRI BT, right) BL, ML, HL and TPW parameters calculated after physical retrieval step profile. In all case the ground truth are the BL, ML, HL and TPW calculated from NWP-Hyb ECMWF analysis (t+00) profiles.*

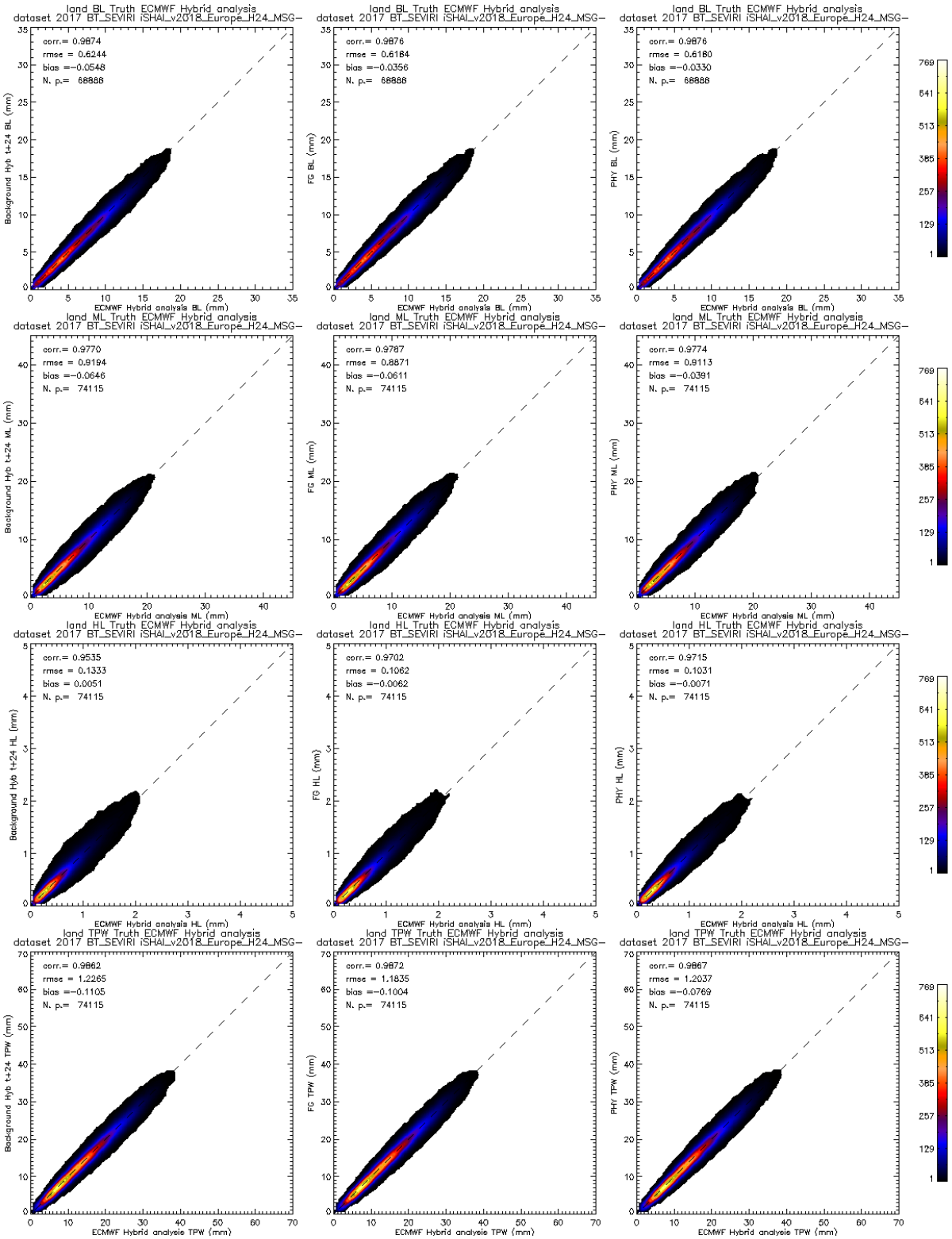

*Figure 33: **BT_SEVIRI** case on Europe region: LPW and TPW 2D histograms over **land** on Europe region validation points of year 2017. From top to bottom BL, ML, HL and TPW parameters. Left) BL, ML, HL and TPW parameters calculated directly from background ECMWF from hybrid profiles from (t+24) forecast, centre) BL, ML, HL and TPW parameters calculated after FG step profile using as input using real bias corrected SEVIRI BT, right) BL, ML, HL and TPW parameters calculated after physical retrieval step profile. In all case the ground truth are the BL, ML, HL and TPW calculated from NWP-Hyb ECMWF analysis (t+00) profiles.*

BL land	NWPHyb (*t+24*)	BT_RTTOV case FG	BT_RTTOV case Phy. Retrieval	BT_SEVIRI case FG	BT_SEVIRI case Phy. Retrieval	BT_SEVIRI_unc case FG	BT_SEVIRI_unc case Phy. Retrieval
RMSE (kg/m^2)	0,624	0,617	0,614	0,618	0,618	0,634	0,638
BIAS (kg/m^2)	-0,055	-0,039	-0,038	-0,033	-0,023	0,076	-0,023
ML land	**NWPHyb (*t+24*)**	**BT_RTTOV case FG**	**BT_RTTOV case Phy. Retrieval**	**BT_SEVIRI case FG**	**BT_SEVIRI case Phy. Retrieval**	**BT_SEVIRI_unc case FG**	**BT_SEVIRI_unc case Phy. Retrieval**
RMSE (kg/m2)	0,919	0,863	0,791	0,887	0,911	0,910	1,011
BIAS (kg/m2)	-0,065	-0,079	-0,075	-0,039	0,000	0,220	0,000
HL land	**NWPHyb (*t+24*)**	**BT_RTTOV case FG**	**BT_RTTOV case Phy. Retrieval**	**BT_SEVIRI case FG**	**BT_SEVIRI case Phy. Retrieval**	**BT_SEVIRI_unc case FG**	**BT_SEVIRI_unc case Phy. Retrieval**
RMSE (kg/m2)	0,133	0,094	0,076	0,106	0,103	0,110	0,105
BIAS (kg/m2)	0,005	0,003	0,000	-0,007	0,064	-0,017	0,064
TPW land	**NWPHyb (*t+24*)**	**BT_RTTOV case FG**	**BT_RTTOV case Phy. Retrieval**	**BT_SEVIRI case FG**	**BT_SEVIRI case Phy. Retrieval**	**BT_SEVIRI_unc case FG**	**BT_SEVIRI_unc case Phy. Retrieval**
RMSE (kg/m2)	1,227	1,153	1,075	1,184	1,204	1,224	1,319
BIAS (kg/m2)	-0,110	-0,112	-0,110	-0,077	0,024	0,273	0,024

Table 14: Statistical parameters for BL, ML, HL and TPW parameters over land Europe validation points in validation (1 out 3 offset 1) year 2017 dataset. Blue column) ECMWF (t+24) Green columns) BT_RTTOV case, light yellow columns) BT_SEVIRI case, red columns) uncorrected bias BT BT_SEVIRI case.

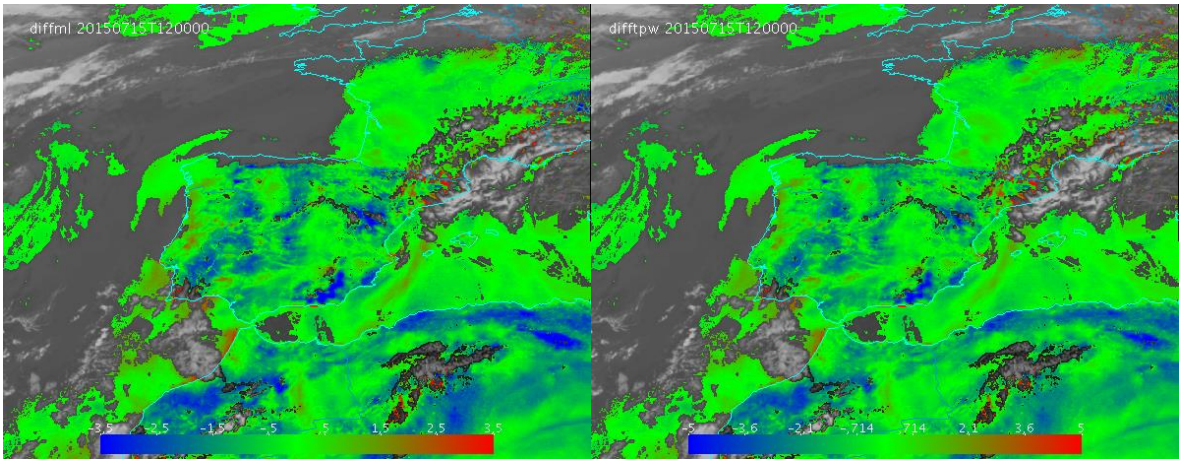

Figure 34: Example of GEO-iSHAI diff_ML and diff_TPW from 12 UTC on 15 July 2015 produced from SEVIRI on MSG-3. Red pixels (large error in ML parameter) in the neighbourhood of cloudy pixels are caused by undetected clouds or cloud contamination.